Lithos 320–321 (2018) 332–354

Contents lists available at ScienceDirect

Lithos

journal homepage: www.elsevier.com/locate/lithos

Probing into Thailand's basement: New insights from U–Pb geochronology, Sr, Sm–Nd, Pb and Lu–Hf isotopic systems from granitoids

Romana E.C. Dew [a,*], Alan S. Collins [a], Stijn Glorie [a], Christopher K. Morley [b,c], Morgan L. Blades [a], Simon Nachtergaele [d], Rosalind King [a], John Foden [a], Johan De Grave [d], Pitsanupong Kanjanapayont [e], Noreen J. Evans [f], Brandon L. Alessio [a], Punya Charusiri [e]

[a] Centre for Tectonics, Resources and Exploration (TRaX), Department of Earth Sciences, The University of Adelaide, Adelaide, South Australia 5005, Australia
[b] PTTEP, EnCo, Soi 11, GGS, Vibhavadi Rangsit Road, Chatuchak, Bangkok 10900, Thailand
[c] Department of Geological Sciences, Chiang Mai University, 239 Huay Kaew Road, Chiang Mai 50200, Thailand
[d] Department of Geology, Ghent University, Krijgslaan 281.S8, WE13, Ghent 9000, Belgium
[e] Basin Analysis and Structural Evolution Special Task Force for Activating Research (BASE STAR), Department of Geology, Faculty of Science, Chulalongkorn University, Bangkok 10330, Thailand
[f] School of Earth and Planetary Science, John de Laeter Centre, TIGeR, Curtin University, Perth, Western Australia 6102, Australia

1. Introduction

The terranes that form Thailand are key to understanding the palaeogeography of Greater Gondwana, the Tethys Oceans and the development of present-day Southeast Asia. In attempts to unravel the tectonic history of Southeast Asia, the region has been divided into various terranes, although there is no consensus on their number, the nature and location of their boundaries, the sources and characteristics of the basement, their global affinities or tectonic models for their amalgamation (Barr et al., 2006; Metcalfe, 2013). This problem is accentuated by the lack of basement exposure due to the vast cover of younger sedimentary sequences, extensive jungle cover and deep lateritic weathering. Therefore, on a regional scale, the nature of the basement within Thailand is mostly unknown. The available basement data is limited to the three main regions of exposure: northern, southeast and on the peninsula (Hansen and Wemmer, 2011). The 'basement' rocks in Thailand, most of which are medium to high grade regional metamorphic rocks, were described as 'Pre-Permian' by Javanaphet (1969). In recent years, radiometric dating yielded basement ages ranging from Cambrian to Paleogene (Kanjanapayont et al., 2012; Kawakami et al., 2014; Lin et al., 2013).

While there are sparse basement exposures, granitoid plutons are common throughout Thailand, and are useful for understanding the nature of the unexposed basement (Charusiri et al., 1993; Cobbing, 2011). These granitoids formed during the stages of subduction and orogenesis (Ng et al., 2015a; Ng et al., 2015b; Searle et al., 2012) and also are part of the Southeast Asian Tin Belt, one of the world's most productive and largest sources of metallic mineral deposits, especially Sn and Cu (Cobbing et al., 1992; Schwartz et al., 1995; Searle et al., 2012). There are two main events that led to this granite emplacement: the Permo-Triassic closure of the Palaeo-Tethys Ocean (and the resultant Indosinian Orogeny) and the Mesozoic–Paleogene closure of the Neo-Tethys Ocean (Gardiner et al., 2016; Searle et al., 2012; Sone and Metcalfe, 2008). The Indosinian Orogeny currently encompasses all late Paleozoic to early Mesozoic orogenesis throughout Asia: from China (Gao et al., 2017; Li et al., 2004), Vietnam (Halpin et al., 2016; Lepvrier et al., 2004), to Thailand (e.g. Barr and Macdonald, 1991; Metcalfe, 2013; Sone and Metcalfe, 2008). However, the precise timing of the individual collisional events that make up the Indosinian Orogeny remains uncertain. The earliest events of the Indosinian Orogeny are latest Permian to Lower Triassic in age and include the collision of South China with Indochina (e.g. Faure et al., 2014). However, the collision of Indochina and Sukhothai terranes with Sibumasu is controversial, and may possibly have been diachronous, with the proposed timing of collision ranging all throughout the Triassic (e.g. Barber et al., 2011; Faure et al., 2014; Hara et al., 2013; Morley et al., 2013; Sone and Metcalfe, 2008).

Isotopic systems provide important information on the crust's evolution and can be spatially modelled to highlight reworked continental crust and juvenile material (Kemp et al., 2006; Liew and McCulloch, 1985). The aim of this study is to use granites as a probe to further develop our understanding of the underlying basement in Thailand. To do this, we use zircon U–Pb geochronology and Lu–Hf isotopic signatures and whole-rock Sr, Pb and Nd geochemistry of granitoids. Together, these signatures assist in unravelling Thailand's complex evolution and help strengthen our understanding of Southeast Asian tectonics.

1.1. Terranes of Thailand

Throughout Thailand, the main tectonic terranes (Sibumasu, Sukhothai and Indochina; Fig. 1) predominantly trend north–south.

* Corresponding author.
E-mail address: romana.dew@adelaide.edu.au (R.E.C. Dew).

https://doi.org/10.1016/j.lithos.2018.09.019

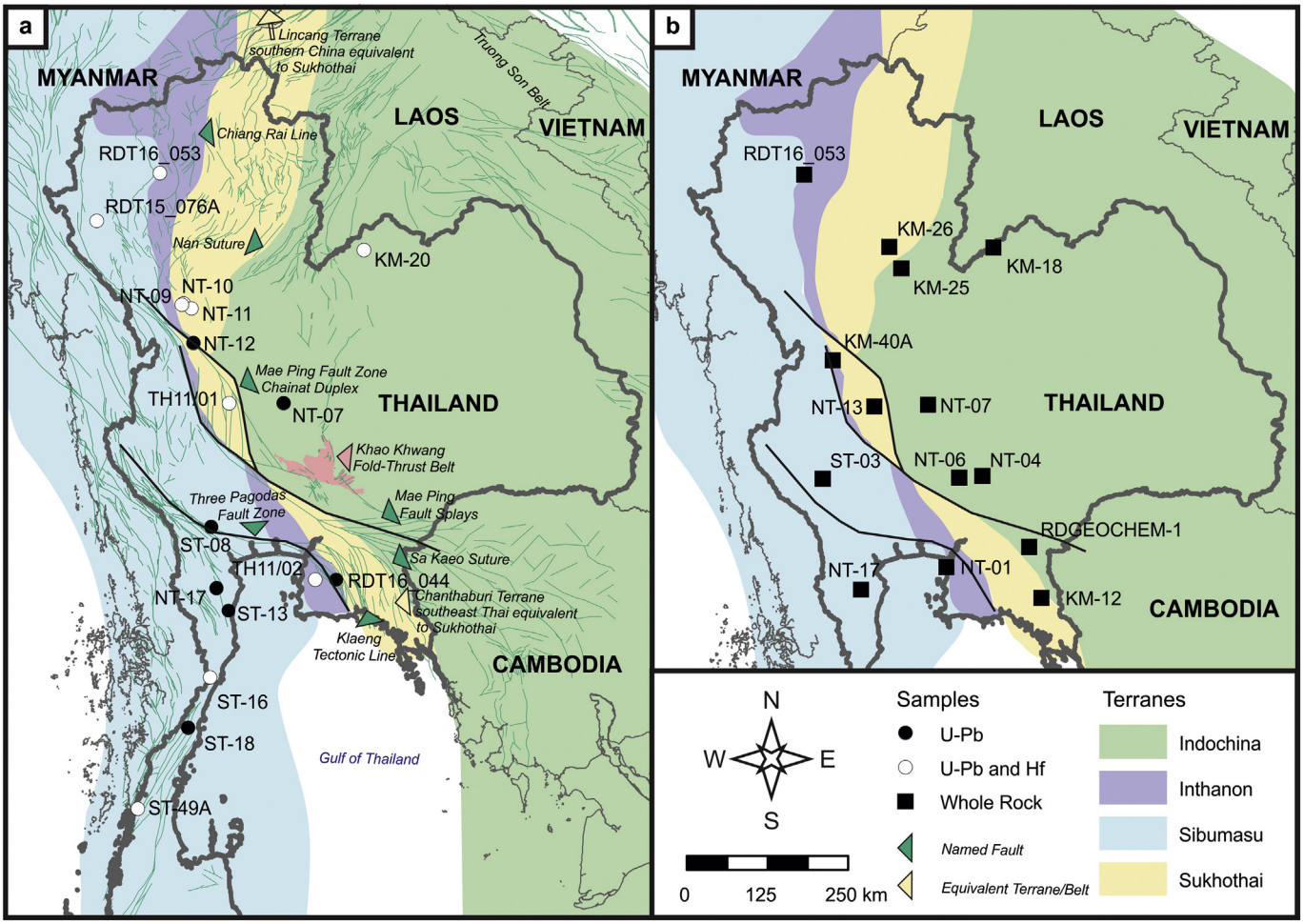

Fig. 1. a (left): Regional map showing major terranes and the granitoid sample localities for zircon U–Pb and Hf analyses. Structure and tectonic domains discussed in text are highlighted with arrows.b (right): Regional map showing major terranes and the granitoid sample localities for whole-rock analyses. Base map adjusted from Dew et al. (submitted) and Sone and Metcalfe (2008).

This trend is not just visible in the main terranes but also in the suture zones, including the Inthanon Zone, coloured purple in Fig. 1.

The Sibumasu Terrane has been variably defined in the past (Audley-Charles et al., 1988; Hisada et al., 2004; Metcalfe, 1984), but here will be defined as the basement of Peninsula Thailand, which extends north into eastern–central Myanmar, east to the Chiang Rai Line and south through the western Malay Peninsula as defined by Gardiner et al. (2016). The name, Sibumasu, is a combination of its constituents: *Si*am-Thailand and *Si*no-China–*Bu*rma–*Ma*laysia–*Su*matra. The Sibumasu Terrane is a ribbon-like continent that is equivalent to the South Qiangtang Terrane in Tibet, and the Baoshan and Tengchong terranes in southwest China (Ali et al., 2013; Jiang et al., 2017). It contains tin-bearing, continental collision S-type granites emplaced between 220 and 200 Ma (Gardiner et al., 2016; Schwartz et al., 1995; Searle et al., 2012). Paleozoic sedimentary rocks, including early Permian glaciomarine diamictites, from the Sibumasu Terrane show Gondwanan biogeographic affinities (Metcalfe, 1984, 2013; Schwartz et al., 1995; Sevastjanova et al., 2011).

The Inthanon Zone represents the convergence zone between the Sukhothai, Indochina and Sibumasu terranes (Hara et al., 2013; Sone and Metcalfe, 2008). It contains deep-water sequences (thought to be remnants of the Palaeo-Tethys Ocean) that have been caught up in an accretionary prism and was subsequently thrust westwards onto the eastern margin of the Sibumasu Terrane (Barber et al., 2011; Barr and Macdonald, 1991; Hara et al., 2012). The Inthanon Zone also contains deformed sequences from the continental margin of the Sibumasu Terrane including metamorphic rocks of unknown age, Cambrian sandstone, Ordovician limestone and Silurian–Carboniferous sedimentary rocks (Hara et al., 2012; Ueno and Charoentitirat, 2011). Barr and Macdonald (1991) introduced the term 'Inthanon Zone' to describe the high grade metamorphic rocks of the Doi Inthanon and Doi Suthep areas, including the detached Paleozoic cover rocks of the Sibumasu Terrane. Usage of this term has since distorted, instead referring to a region containing relics of the Palaeo-Tethys oceanic domain (see Fig. 1).

The Sukhothai Terrane is thought to be equivalent to the Chanthaburi Terrane in southwest Thailand and the Lincang Terrane of southern China (Fig. 1; Sone and Metcalfe, 2008). This region contains the remnants of an arc and its associated short-lived basin (e.g. Metcalfe, 2013; Sone and Metcalfe, 2008). The Sukhothai Terrane is dominated by a Permo-Triassic deformed fore-arc basin sequence and overlying late Permian–Triassic shallow marine molasse-type sedimentary rocks (Chaodamrong, 1992; Hara et al., 2017). The Sukhothai Terrane also includes Permo-Triassic metaluminous granitoids with an I-type affinity (Sone et al., 2012; Sone and Metcalfe, 2008). Indosinian-aged deformation occurred in the "Sukhothai Fold Belt", with the resultant cleavage giving a K–Ar age between 220 and 188 Ma (Ahrendt et al., 1993). During the Carboniferous and Permian, the Nan basin has been interpreted to have separated the Sukhothai and Indochina terranes (Barr and Macdonald, 1987; Qian et al., 2016; Sone and Metcalfe, 2008; Ueno and Hisada, 2001). This, supposedly, short-lived back-arc basin, is preserved as a narrow N–S trending and discontinuous ophiolite belt known as the Nan–Uttaradit Suture in northern Thailand and Sa Kaeo Suture in the southeast of the country (Fig. 1; Sone and Metcalfe, 2008; Ueno and Hisada, 2001). This suture zone is a mélange

complex of gabbro (zircon U–Pb age of 311 ± 10 Ma), tholeiitic metabasalt (zircon U–Pb age of 316 ± 3 Ma), andesite and radiolarian chert lithologies (Barr and Macdonald, 1987; Sone et al., 2012).

The Indochina Terrane extends across large expanses of Laos, Vietnam, Cambodia, Malaysia and Thailand (Fig. 1). There is evidence that it may be a composite terrane comprised of multiple micro-terranes, potential sutures, metamorphic complexes and mylonitic fault zones (Lepvrier et al., 2004; Sone and Metcalfe, 2008). Within Thailand, the Indochina Terrane encompasses all of Thailand east of the Sukhothai Terrane. The granitoids from the Indochina Terrane are mostly metaluminous I-type granitoids that are related to Cu–Fe–Au–Sb mineralisation (Charusiri et al., 1993; Salam et al., 2014; Zaw et al., 2014). Mesozoic and Cenozoic sediments cover the Indochina Terrane throughout most of Thailand, however basement rocks, up to granulite-facies, are exposed in Vietnam, Laos and Cambodia (Nakano et al., 2018; Shi et al., 2015; Wang et al., 2016b). Model ages and inherited zircons suggest that the main crust of the Indochina Terrane formed in the Paleoproterozoic to Mesoproterozoic (Lan et al., 2003; Shi et al., 2015; Wang et al., 2016b). There is evidence that the high grade metamorphism of basement rocks such as the Kontum Massif and the Truong Son Belt were caused by the multi-phased Indosinian Orogeny, often specifically attributed to the oblique collision of the Indochina and South China terranes (see Halpin et al., 2016; Lan et al., 2003; Lepvrier et al., 2004; Nakano et al., 2018). However, no data are available on the nature of the buried Indochina basement that underlies eastern Thailand.

1.2. Proterozoic to Triassic tectonic evolution

Previous studies have located the Indochina and Sibumasu terranes within the Gondwana supercontinent during the Proterozoic to early Paleozoic, with Sibumasu off the margin of northern Australia and Indochina further outboard (Bunopas, 1981; Burrett et al., 2014; Cocks and Torsvik, 2013; Usuki et al., 2013). In the past, there has been much debate on the origin of Sukhothai Terrane, however, it is now acknowledged to be an arc system built on older continental material (Hara et al., 2017; Sevastjanova et al., 2011).

The northern Gondwana margin was tectonically dynamic in the Cambro-Ordovician, when strike-slip faulting caused Indochina and South China to begin moving eastwards (Cocks and Torsvik, 2013). Indochina, South China and northern Tibet separated from Sibumasu and other remnants of Gondwana as the southern Palaeo-Tethys Ocean opened in the Lower Devonian (Cocks and Torsvik, 2013; Hara et al., 2012; Metcalfe, 2013). This ocean covered the equatorial region from the Devonian to the Triassic, where carbonates and pelagic chert were deposited (Cocks and Torsvik, 2013; Hara et al., 2012; Metcalfe, 2013). The preserved Palaeo-Tethyan rocks are characterised by ocean plate stratigraphy, and were later subducted during the Permian–Triassic under the Indochina Terrane (Cai et al., 2017; Metcalfe, 2013; Wakita and Metcalfe, 2005).

Previously published plate-tectonic models (e.g. Li et al., 2004; Metcalfe, 2013) suggest that by the Carboniferous, the South China and Indochina terranes were located in equatorial to low northern palaeolatitudes. The Indochina Terrane became a stable carbonate shelf in the middle Carboniferous (Ueno and Charoentitirat, 2011). By the late Carboniferous, carbonate platforms developed along the margin of the Indochina Terrane (Dew et al., (submitted); Ueno and Charoentitirat, 2011; Wielchowsky and Young, 1985). Rift-grabens filled with glacial-marine sediments derived from Gondwana, indicate that during the early Permian, the Sibumasu Terrane rifted from the Himalayan-Australian margin of Gondwana (Burrett et al., 2014; Metcalfe, 2013). This northward movement of the Sibumasu Terrane is thought to have opened the Meso-Tethys Ocean (Burrett et al., 2014). The late Carboniferous–early Permian sparked the start of the destruction of the main Palaeo-Tethys Ocean, with subduction northwards beneath the Indochina Terrane (Li et al., 2004; Metcalfe, 2013; Sone et al., 2012). In this model, as subduction continued, slab rollback caused the Nan back-arc basin to open between the Indochina and the Sukhothai terranes (Metcalfe, 2013). Subduction of the Palaeo-Tethys Ocean formed an accretionary wedge of "ocean plate stratigraphy" and caused the arc magmatism of the Sukhothai Terrane (Barr et al., 2006; Qian et al., 2016).

The Indosinian Orogeny led to granite emplacement throughout much of Thailand, often described as the Central/Main Range and Eastern Granitoid Provinces (Cobbing, 2011; Searle et al., 2012). The timing of the collision between Indochina and Sibumasu is yet to be detailed, and current constraints range from latest Permian to late Triassic (Barber et al., 2011; Cai et al., 2017; Hara et al., 2012; Metcalfe, 2013; Wakita and Metcalfe, 2005). The early stage of this orogenic event is thought to be driven by the collision of northern margin of the Indochina Terrane with the South China Terrane (Arboit et al., 2014; Lepvrier et al., 2004; Metcalfe, 2013; Morley et al., 2013). Contemporaneously, or following the South China–Indochina terrane collision, the Nan basin closed and subsequently thrust the Sukhothai Terrane over the Indochina Terrane (Lepvrier et al., 2004; Morley et al., 2013). On the southern margin of the Khorat continental fragment of the Indochina Terrane, the Khao Khwang Platform was deformed resulting in the Khao Khwang Fold-Thrust Belt (Arboit et al., 2016; Dew et al., (submitted); Morley et al., 2013; Sone and Metcalfe, 2008). The age of this collision, which was possibly related to the closure of a small oceanic basin between different Indochina Terrane fragments, is marked by granite emplacement at a peak age of ~241 Ma (Meffre et al., 2008). In the Khorat Plateau of central Thailand, the end of this early Indosinian event (sometimes known as *Indosinian I)* is defined by an unconformity whereby the deformed Permian and older units are overlain by late Triassic (~220 Ma) Kuchinarai Group rift-related sediments (Booth and Sattayarak, 2011). The later Indosinian Orogeny (referred to as the *Indosinian II* event) is thought to be related to the collision of the Sibumasu Terrane to the Sukhothai and Indochina terranes (Booth and Sattayarak, 2011; Morley et al., 2013). The sediments of the Sibumasu Terrane were thrust underneath the accretionary complex of the Sukhothai Terrane with the closure of the subduction zone (Sone and Metcalfe, 2008).

2. Methodology

2.1. Sample acquisition

Twenty-eight granitoid samples in total are used for this study. The sampling strategy for this study was to collect granitoids from all three terranes and across major faults and sutures to better delineate tectonic boundaries. Representative samples of granitoids, and therefore also their underlying basement, were collected from widespread localities within Thailand. The individual sample locations and lithology and analysis method for each sample are outlined in Table 1. For further details on the sample preparation and petrographic descriptions see Dew et al. (submitted).

2.2. U–Pb zircon geochronology

Eighteen granitoid rock samples were used for zircon analyses. Details of the preparatory methods and analytical conditions are summarized by Dew et al. (submitted). All cathodoluminescence (CL) imagery and laser ablation inductively coupled plasma mass spectrometry (LA–ICP–MS) was completed at Adelaide Microscopy, Adelaide, South Australia. The GEMOC zircon standard GJ-1 ($^{206}Pb/^{238}U$ TIMS age of 600.7 ± 1.1 Ma) was run as the primary standard every 10–20 unknown analyses, to correct for isotopic drift and down-hole fractionation. Across all analytical sessions, analyses of GJ-1 yielded a $^{206}Pb/^{238}U$ weighted average age of 601.61 ± 0.47 Ma ($n = 556$, MSWD = 1.10). For further information on the zircon standards, analytical parameters and reduction techniques, see Dew et al. (submitted).

Table 1
Descriptions and localities for samples in this study.

Sample Name	Latitude	Longitude	Lithology	Mineralogy	Previous description or affinity	Interpreted U–Pb Age (Ma)	Age Source	Lu–Hf	Sr, Sm–Nd	Pb
KM-12	12°54′38.52”N	102°14′29.58″E	granodiorite	Holocrystalline Qtz + Pl + Kfs + Bt + Mu + Chl	Eastern Province Late Triassic I-type granite (on Kawakami et al., 2014 map)	217 ± 3	Nearby Th 18/95 (Hansen and Wemmer, 2011)		x	
KM-18	17°47′12.18”N	101°34′34.08″E	qtz-diorite	Holocrystalline, equigranular Qtz + Pl + Hbl + Px	Mapped as a granodiorite by Intasopa and Dunn (1994) Eastern Granitoid Province	229.9 ± 1.9	Nearby U–Pb data KM-20		x	
KM-20	17°43′53.34”N	101°47′4.14″E	granodiorite	Holocrystalline Qtz + Pl + Kfs	Eastern Granitoid Province	229.9 ± 1.9	Weighted average $^{206}Pb/^{238}U$ age This Study	x		
KM-25	17°29′40.08”N	100°18′7.20″E	tonalite	Holocrystalline Qtz + Pl + Kfs + Bt + Chl + Mu + Sill + Ep	Eastern Granitoid Province	296 ± 20	Nearby U–Pb age by (Meffre et al., 2008b)		x	x
KM-26	17°47′31.98”N	100° 7′48.30″E	tonalite	Holocrystalline Qtz + Pl + Bt + Chl + Cpx + Mu + Sill + Sp	Eastern Granitoid Province	296 ± 20	Nearby U–Pb age by (Meffre et al., 2008b)		x	x
KM-40A	16°12′57.18”N	99°16′42.84″E	granite	Holocrystalline Qtz + Kfs + Pl + Bt + Chl + Mu		238.0 ± 2.9	Nearby U–Pb data NT-12		x	x
NT-01	13°20′22.50”N	100°55′28.80″E	biotite granite	Holocrystalline Bt + Qtz + Kfs + Pl + Chl + Mu	Main Range Granitoid Province	229 + 21/−27	Nearby sample Th 22/95 (Hansen and Wemmer, 2011)		x	x
NT-04	14°36′29.50”N	101°25′21.90″E	quartz diorite	Holocrystalline Qtz + Pl + Kfs + Sp + Hbl + To	Eastern Granitoid Province	241 ± 6	Nearby Pak Chong granodiorite age quoted by Arboit et al. (2016)		x	
NT-06	14°34′56.40”N	101° 6′13.40″E	amphibolitic gabbro-diorite	Holocrystalline Hbl + Pl + Kfs + Chl + Sp	Eastern Granitoid Province	241 ± 6	Nearby Pak Chong granodiorite age quoted by Arboit et al. (2016)		x	
NT-07	15°35′57.10”N	100°40′9.80″E	quartz diorite	Holocrystalline, porphyritic-phaneritic Qtz + Pl + Hbl + Kfs + Chl + Mu	Eastern Granitoid Province	273.5 ± 3.9	Weighted average $^{206}Pb/^{238}U$ age This Study		x	
NT-09	16°59′32.90”N	99°16′34.90″E	diorite-monzonite	Holocrystalline Pl + Kfs + Hbl + Qtz + Chl + Bt + Mu	Tak Batholith	226.5 ± 1.8	Weighted average $^{206}Pb/^{238}U$ age This Study	x		
NT-10	16°59′32.90”N	99°16′34.90″E	(leuco)granite	Holocrystalline Qtz + Kfs + Pl + Bt + Chl	Tak Batholith	236.2 ± 2.9	Discordia lower intercept This Study	x		
NT-11	16°55′16.10”N	99°23′19.00″E	granite	Holocrystalline Qtz + Kfs + Bt + Sp + Ep	Tak Batholith	228.7 ± 2.1	Weighted average $^{206}Pb/^{238}U$ age This Study	x		
NT-12	16°26′12.20”N	99°24′49.80″E	granodiorite	Holocrystalline Qtz + Pl + Kfs + Chl + Bt + Mu + Gt	Tak Batholith	238.0 ± 2.9	Weighted average $^{206}Pb/^{238}U$ age This Study			
NT-13	15°34′28.20”N	99°55′0.80″E	granite-adamellite	Holocrystalline Qtz + Kfs + Pl + Bt + Mu + Gt		227.9 ± 1.9	Nearby U–Pb data Th11/01		x	x
NT-17	13° 1′23.00”N	99°44′11.30″E	granite	Holocrystalline, porphyritic-phaneritic Qtz + Kfs + Mu + Pl	Mogok–Mandalay–Mergui Belt	214.15 ± 0.87	Weighted average $^{206}Pb/^{238}U$ age This Study		x	x

(continued on next page)

Table 1 (*continued*)

Sample Name	Latitude	Longitude	Lithology	Mineralogy	Previous description or affinity	Interpreted U–Pb Age (Ma)	Age Source	Lu–Hf	Sr, Sm–Nd	Pb
RDT15_076A	18° 9′5.00”N	98° 4′7.00″E	altered granodiorite	Holocrystalline, Pl + Qtz + Mu + Fl	Similar to Mae Lama pluton	No crystallisation identified	Inherited ages only	x		
RDT16_044	13°10′12.00”N	101°24′2.00″E	migmatite	Holocrystalline, banded Qtz + Pl + Mu + Gt + Hbl + Chl	Mylonitic gneiss (Kawakami et al., 2014)	73.3 ± 3.7	$^{206}Pb/^{238}U$ age of youngest near concordant zircon This Study			
RDT16_053	18°48′4.00”N	98°56′47.48″E	adamellite	Holocrystalline Qtz + Pl + Kfs + Bt + Chl		204.1 ± 1.6	Weighted average $^{206}Pb/^{238}U$ age This Study	x	x	x
RDGEOCHEM-1	13°37′05”N	102°4′47″E	granodiorite	Holocrystalline, perthitic textures Qtz + Kfs + Pl + Mc + opaques	Late Triassic I-type granite (on Kawakami et al. 2014 map) Eastern Granitoid Province	203 ± 8	Nearby U–Pb data by Muller et al. (1999) collated by Zaw et al. (2014)		x	
ST-03	14°34′5.10”N	99°12′13.90″E	granodiorite with tourmaline pegmatite	Holocrystalline Qtz + Pl + Bt + Mu + To	Mogok–Mandalay–Mergui Belt	213.6 ± 2.9	Nearby U–Pb data ST-08A		x	
ST-08A	13°52′32.60”N	99°39′50.70″E	(grano)diorite	Holocrystalline, phaneritic Pl + Kfs + Qtz + Bt + Hbl + Chl + Mu	Mogok–Mandalay–Mergui Belt	213.6 ± 2.9	Weighted average $^{206}Pb/^{238}U$ age This Study			
ST-13	12°42′27.40”N	99°54′7.60″E	granite	Holocrystalline Kfs + Qtz + Pl + Bt	Hub Kapong Kawakami 2014	210.9 ± 1.1 (magmatic) 80.72 ± 0.79 (metamorphic)	Weighted average $^{206}Pb/^{238}U$ ages This Study			
ST-16	11°47′23.60”N	99°38′56.10″E	granite	Holocrystalline Kfs + Qtz + Pl + Bt + Chl + Mu	Mogok–Mandalay–Mergui Belt DeClerq 2016	501 ± 15	Weighted average $^{206}Pb/^{238}U$ age This Study	x		
ST-18	11° 5′5.00”N	99°20′20.00″E	granodiorite	Holocrystalline Qtz + Pl + Kfs	Mogok–Mandalay–Mergui Belt DeClerq 2016	76.26 ± 0.82	Weighted average $^{206}Pb/^{238}U$ age This Study			
ST-49A	9°57′32.80”N	98°38′37.20″E	granite	Holocrystalline Kfs + Qtz + Mu + Pl + Chl + Mu + Gt	Mogok–Mandalay–Mergui Belt	81.4 ± 1.1	Weighted average $^{206}Pb/^{238}U$ age This Study	x		
TH11/01	15°36′2.52”N	99°54′49.91″E	granite	Holocrystalline Kfs + Pl + Qtz		227.9 ± 1.9	Weighted average $^{206}Pb/^{238}U$ age This Study	x		
TH11/02	13° 8′49.66”N	101° 6′43.01″E	granite	Holocrystalline Kfs + Qtz + Mu + Pl	Main Range Granitoid Province	206.4 ± 1.4	Weighted average $^{206}Pb/^{238}U$ age This Study	x		

Mineral abbreviations are as follows: quartz (Qtz), plagioclase (Pl), K-feldspar (Kfs), microcline (Mc), pyroxene (Px), clinopyroxene (Cpx), orthopyroxene (Opx), hornblende (Hbl), biotite (Bt), muscovite (Mu), garnet (Gt), chlorite (Chl), sillmanite (Sill), tourmaline (To), epidote (Ep), sphene (Sp) and fluorite (Fl).For further petrographic information, see in-table references and Dew et al. (submitted).All age uncertainties where given are 2σ.

2.3. Zircon Lu–Hf isotope analysis

After the U–Pb zircon geochronology analyses, ten of these granitoid samples were selected for further zircon Lu–Hf isotope analysis. A subset of the zircon grains for each sample were then analysed for their hafnium isotopic composition (for grain specific information see Table 4 of Dew et al. submitted). The number of Hf analyses for each sample was determined by the variability in the age data and the amount of interpreted inheritance. For individual zircon U–Pb ages that were interpreted to be indicative of the overall granitoid crystallisation age, the weighted average age of the granitoid was used to calculate the initial $^{176}Hf/^{177}Hf$. For interpreted inherited zircons the age of the individual analysis was used to calculate the initial $^{176}Hf/^{177}Hf$. Nine samples used for Hf and Lu isotopic analyses (all samples except KM-20) were analysed using a Resonetics S-155-LR 193 nm excimer laser ablation system connected to a Nu Plasma II multi-collector ICP–MS in the GeoHistory Facility, John de Laeter Centre, Curtin University, Perth, Western Australia. Hafnium analysis for one sample (KM-20) was undertaken using a Neptune Plus multi-collector ICP–MS at the University of Wollongong, New South Wales. For further information on standards, analytical parameters, correction and reduction techniques, see Dew et al. (submitted).

2.4. Sm–Nd, Sr and Pb whole-rock geochemistry

Sm–Nd and Sr isotopic whole-rock analyses were conducted for fourteen granitoid samples and one duplicate run for Sm–Nd analyses (NT-13) at the University of Adelaide's Isotope Geochemistry Facility (see Table 1). Eight samples and one duplicate (NT-13) were used for whole-rock Pb isotope measurements (see Table 1). These samples were chosen due to their spatial distribution across the main tectonic terranes in Thailand (see Fig. 1), and also containing Nd, Sr and Pb elemental concentrations above the detection limits of the X-ray fluorescence spectrometer (XRF) at Franklin and Marshall College, U.S.A. Details of analytical conditions, standards and sample preparation are summarized in Dew et al. (submitted).

3. Results

3.1. U–Pb zircon geochronology

The age of the granitoids in Thailand is mostly well constrained (Cobbing, 2011; Hansen and Wemmer, 2011; Salam et al., 2014; Searle et al., 2012). Additional granitoid ages have been determined in this study, specifically to better constrain the isotopic data collected (Lu–Hf, Sr, Sm–Nd and Pb) for their age, and to target any inherited components.

The morphologies and internal structure of the zircons analysed using LA–ICP–MS are documented in Fig. 2. Concordia plots were created using Isoplot (Ludwig, 1998), and are displayed in Fig. 3. The crystallisation ages are interpreted from data within ±5% discordance using the ($^{206}Pb/^{238}U$ age)/ $^{207}Pb/^{235}U$ age) calculation. Some analyses clearly show the effects of radiogenic lead loss with anomalously young apparent $^{206}Pb/^{238}U$ ages. Crystallisation ages from these samples were also determined using regression techniques where appropriate. Outliers were rejected after subsequent examination, if the laser beam traversed cracks or overlapped with multiple zircon domains within the grain. For further information on the U–Pb LA–ICP–MS data, see Dew et al. (submitted).

3.1.1. Sibumasu Terrane

Crystallisation ages for granitoids from the Sibumasu Terrane vary from the Cambrian to the Cretaceous. The interpreted crystallisation age for ST-16 was the weighted average age of the cluster of concordant analyses yielding a $^{206}Pb/^{238}U$ age of 501 ± 15 Ma ($n = 4$, MSWD = 1.4; Fig. 3, Dew et al. submitted Table 4). Analyses from ST-16 that were younger than Cambrian in age had very low Th:U, suggesting that the large Th ion has diffused from the zircon during a subsequent thermal event. The observation that young $^{206}Pb/^{238}U$ age zircons have low Th/U ratios suggests that both Pb and Th have been lost from the zircon. This is supported by petrographic observations of igneous garnet breaking down to muscovite, chlorite and biotite (Dew et al. submitted, Fig. 1—mm, nn). The interpreted crystallisation age for NT-17 is the weighted average of the cluster of concordant (±5%) analyses yielding a $^{206}Pb/^{238}U$ age of 214.15 ± 0.87 Ma ($n = 10$, MSWD = 0.89; Fig. 3). For ST-08A, concordant (±5%) analyses all with Th:U > 0.19 yielded a weighted average $^{206}Pb/^{238}U$ age of 213.6 ± 2.9 Ma ($n = 9$, MSWD = 3.1; Fig. 3). The crystallisation age of ST-13 was determined from the concordant (±5%) analyses all with Th:U > 0.1, which yielded a weighted average $^{206}Pb/^{238}U$ age of 210.9 ± 1.1 Ma ($n = 23$, MSWD = 1.2). A younger cluster of data with low Th:U was interpreted to be the age of metamorphic resetting, yielding a weighted average $^{206}Pb/^{238}U$ age of 80.72 ± 0.79 Ma ($n = 5$, MSWD = 0.58). The crystallisation age of ST-49A was determined from the cluster of concordant (±5%) data analyses yielding a $^{206}Pb/^{238}U$ age of 81.4 ± 1.1 Ma ($n = 6$, MSWD = 0.37). The interpreted crystallisation age for ST-18 was determined by the weighted average of concordant (±5%) zircon analyses, yielding a $^{206}Pb/^{238}U$ age of 78.26 ± 0.82 Ma ($n = 10$, MSWD = 1.5; Fig. 3).

Analyses from RDT15_076A included many inherited ages with no crystallisation age evident in the data collected (see Figs. 2 and 3). Interpreted inherited zircon analyses from the Sibumasu Terrane ranged in age from $^{207}Pb/^{206}Pb$ age of 3189.3 ± 17.8 Ma to $^{206}Pb/^{238}U$ age of 371.5 ± 5.8 Ma, with age peaks at 2725 Ma, 2491 Ma, 1360 Ma, 1090 Ma, 940 Ma, 840 Ma, 700 Ma and 500 Ma (see Fig. 3). For further details on the age determination, please see Dew et al. (submitted).

3.1.2. Inthanon Zone

Three samples from the Inthanon Zone were analysed for U–Pb zircon geochronology. Concordant (±5%) zircon analyses from Th11/02 with Th:U > 0.1 yield a tightly constrained age magmatic age of 206.4 ± 1.4 Ma ($n = 22$, MSWD = 0.47, Fig. 3). The interpreted crystallisation age for RDT16_053 is the weighted average of all concordant (±5%) analyses with Th:U > 0.1, yielding a $^{206}Pb/^{238}U$ age of 204.1 ± 1.6 Ma (MSWD = 1.15, $n = 4$). The interpreted crystallisation age for RDT16_044 is the youngest concordant grain yielding a $^{206}Pb/^{238}U$ age of 73.3 ± 3.7 Ma. The Th:U of this zircon is >0.1 however, the majority of the analyses from this sample have low Th:U indicating that both Pb and Th have been lost from the zircon during subsequent thermal events. The interpreted inherited analyses ranged from a $^{207}Pb/^{206}Pb$ age of 2746 ± 29 Ma to a $^{206}Pb/^{238}U$ age of 258.8 ± 4.2 Ma (see Fig. 3). There is a concentration of middle Permian ages from interpreted inherited ages from the Inthanon Zone samples with an age peak at 270 Ma.

3.1.3. Sukhothai Terrane

No concordant inherited zircons were found from any of the five samples from the Sukhothai Terrane (coloured yellow in Fig. 3). The interpreted crystallisation age for NT-12 is the weighted average of all seven concordant (±5%) analyses yielding a $^{206}Pb/^{238}U$ age of 238.0 ± 2.9 Ma (MSWD = 0.95; Fig. 3). The interpreted crystallisation age for NT-10 is the weighted average of all seven concordant (±5%) zircon analyses yielding a $^{206}Pb/^{238}U$ age of 238.6 ± 2.9 Ma ($n = 7$, MSWD = 0.88; Fig. 3). Nineteen concordant (±5%) analyses from NT-11 have Th:U > 0.1 and yield a $^{206}Pb/^{238}U$ weighted average age of 228.7 ± 2.1 Ma (MSWD = 0.48; Fig. 3). The magmatic age of Th11/01 is interpreted to be the weighted average of the ±5% concordant analyses with Th:U > 0.1 yielding a $^{206}Pb/^{238}U$ age of 227.9 ± 1.9 Ma ($n = 23$, MSWD = 1.2; Fig. 3). Concordant (±5%) analyses with Th:U > 0.1 from sample NT-09 yielded a weighted average $^{206}Pb/^{238}U$ age of 226.5 ± 1.8 Ma ($n = 18$, MSWD = 0.48; Fig. 3). This range of Triassic magmatic ages

Fig. 2. Representative cathodoluminescence images for all granitoid rocks sampled in Thailand. U–Pb laser, Hf spots shown.The age given for each spot is the U^{238}/Pb^{206} age, unless marked with an asterisk (*) indicating that the Pb^{207}/Pb^{206} Age is given. Individual spot $\varepsilon Hf_{(t)}$ values are given.

are common in the "Eastern Granitoid Province" within the Sukhothai and Indochina terranes (Charusiri et al., 1993; Searle et al., 2012).

3.1.4. Indochina Terrane

KM-20 contains $^{206}Pb/^{238}U$ ages within 5% discordance for the entire first half of the Triassic period, from 249.4 ± 5.9 Ma to 221.5 ± 5.7 Ma. All zircons analyses contained Th:U >0.4. We interpret that the ages older than 235.5 Ma are inherited and the crystallisation age was calculated from the weighted average of all concordant (±5%) zircon analyses younger than 235.5 Ma, yielding a $^{206}Pb/^{238}U$ age of 229.9 ± 1.9 (n = 18, MSWD = 1.9). All zircons analyses from NT-07 contained Th:U >0.61. The weighted average of 273.5 ± 3.9 Ma (n = 5, MSWD = 2.6)

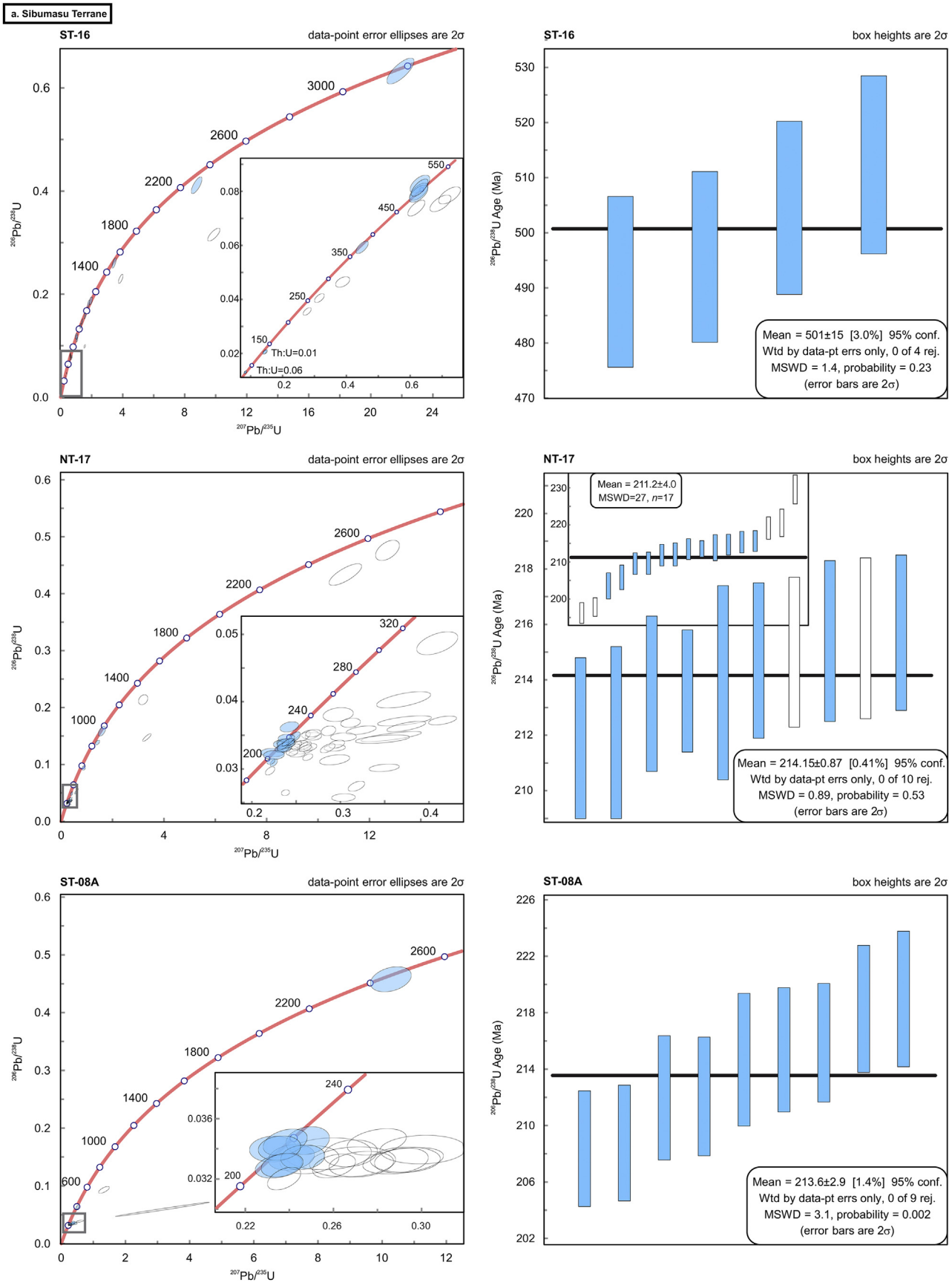

Fig. 3. Concordia diagrams and weighted averages for each U–Pb sample, grey box indicates extent of expanded concordia where applicable.All age uncertainties are quoted at the two sigma level and MSWDs are quoted for each calculated age. a: U–Pb data for samples from the Sibumasu Terrane, coloured blue, b: U–Pb data for samples from the Inthanon Zone, coloured purple,. c: U–Pb data for samples from the Sukhothai Terrane, coloured yellow-orange, d: U–Pb data for samples from the Indochina Terrane, coloured green. Data with Th:U < 0.1 are coloured white on the weighted average plots.

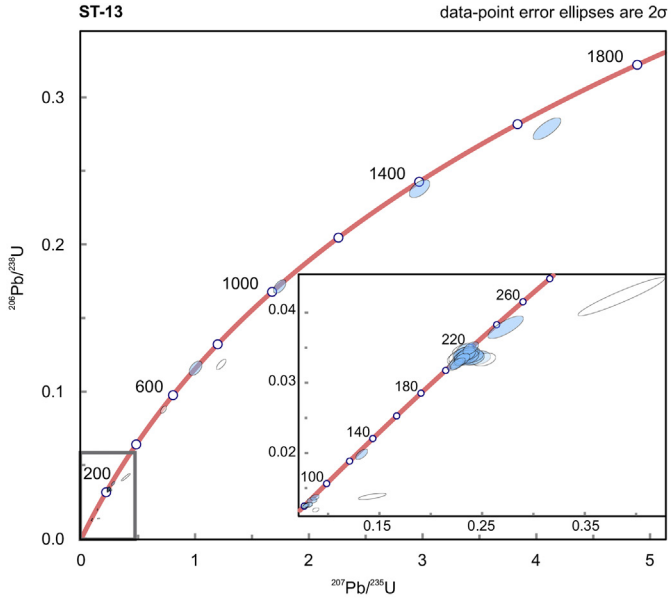

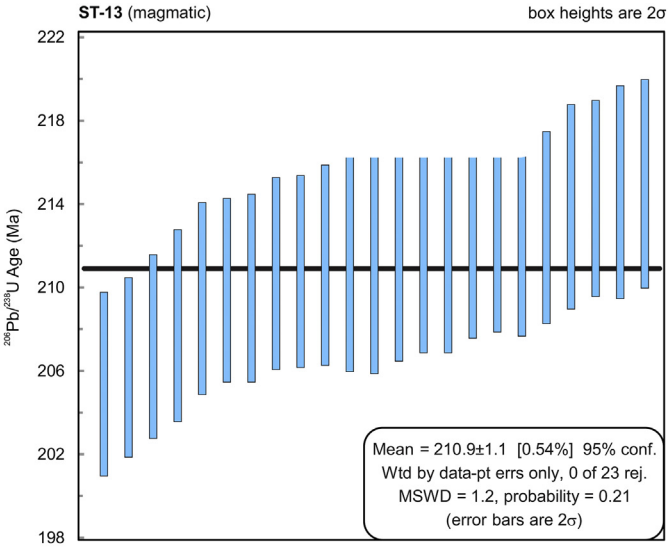

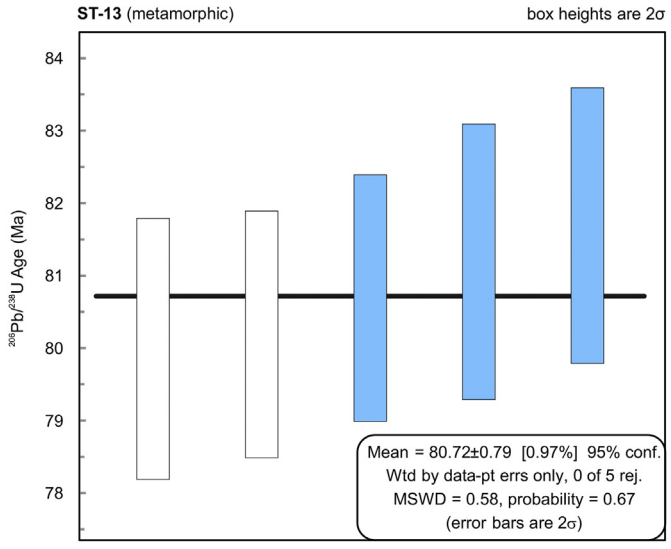

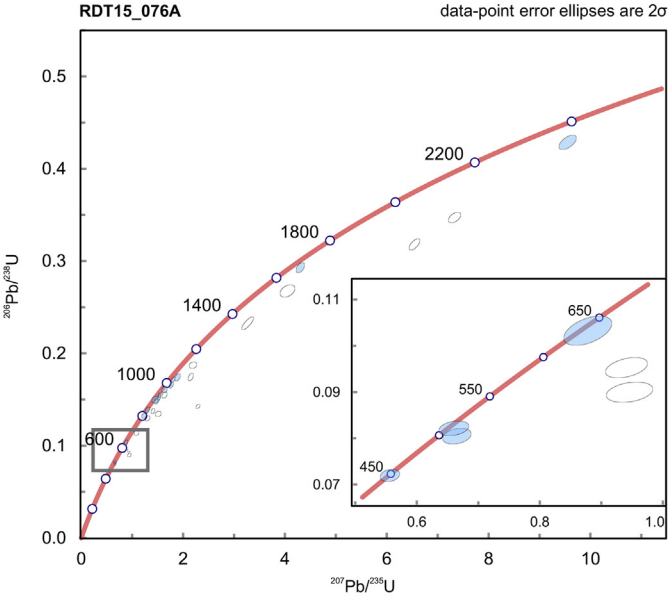

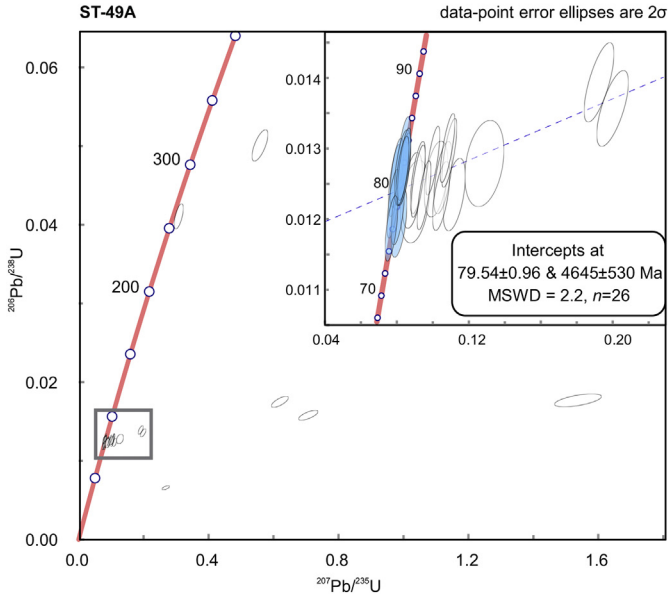

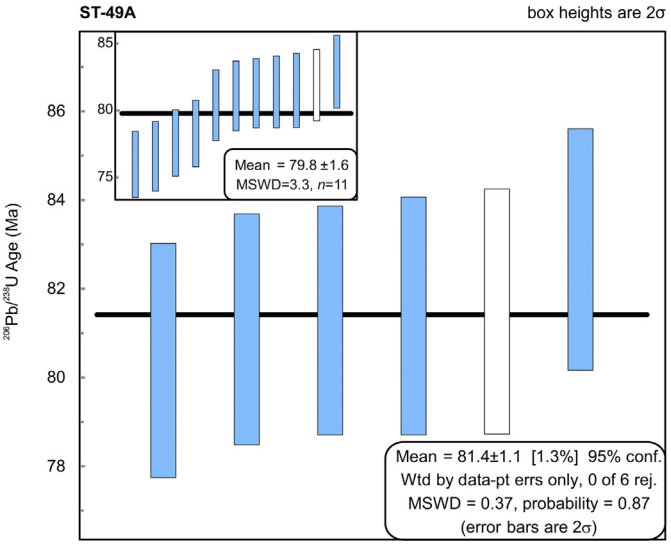

Fig. 3 *(continued).*

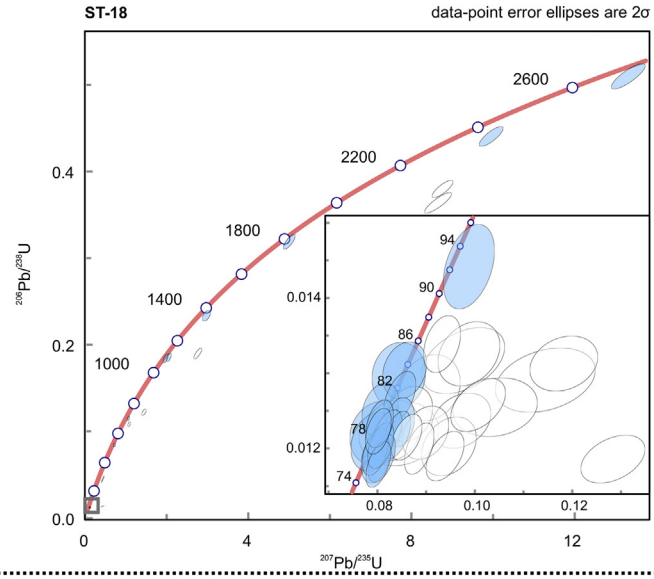

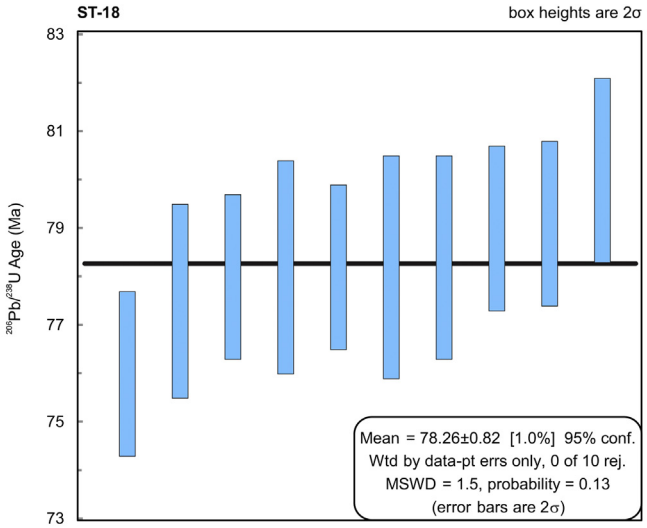

b. Inthanon Zone

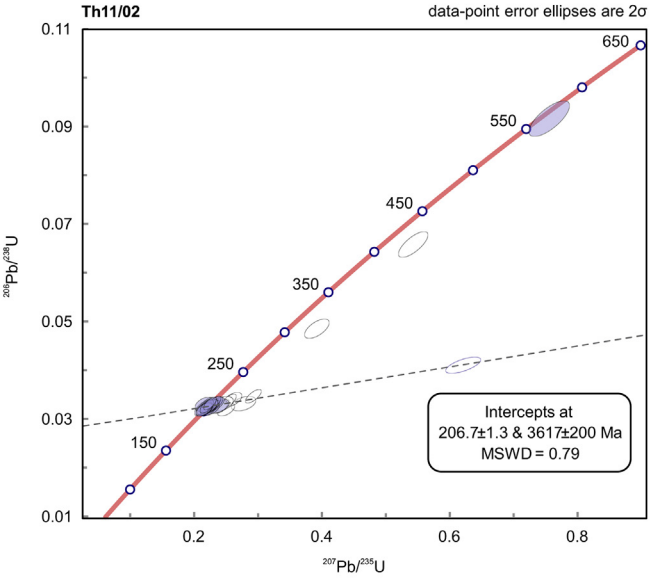

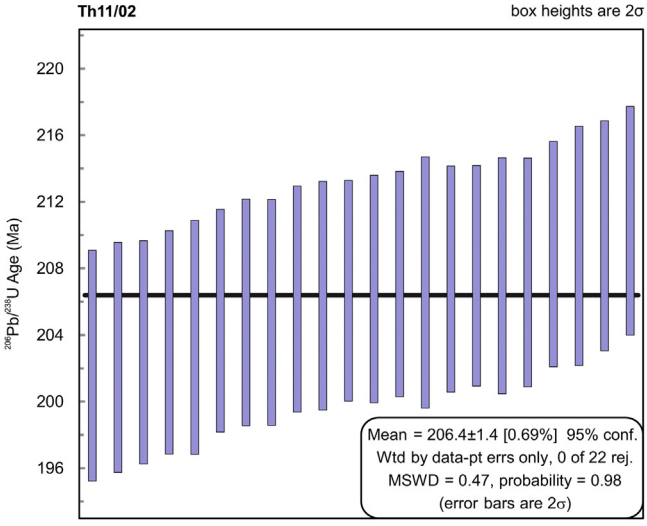

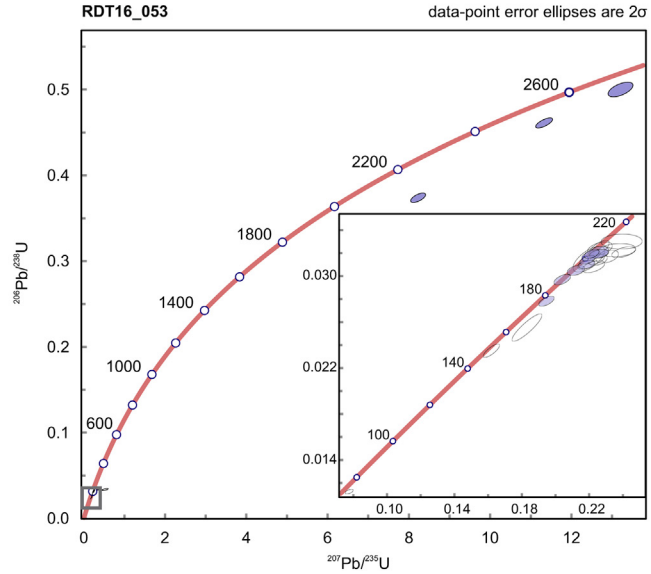

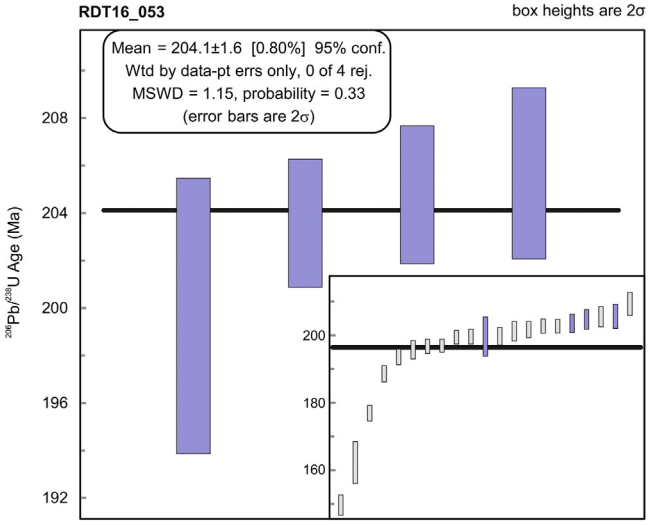

Fig. 3 *(continued)*.

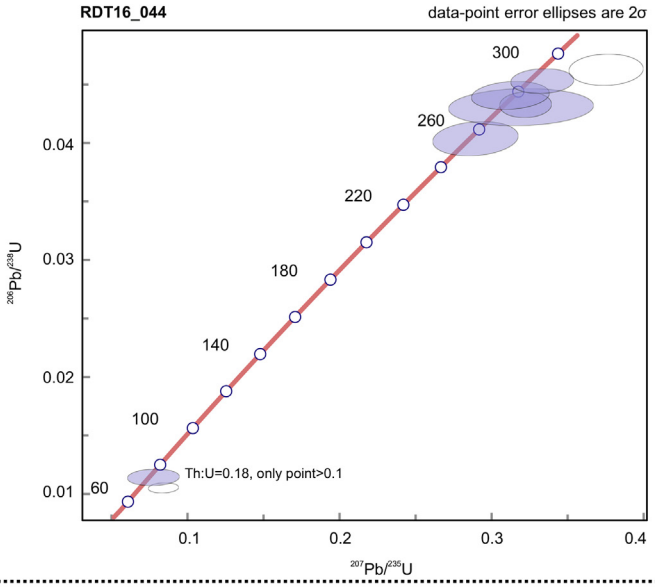

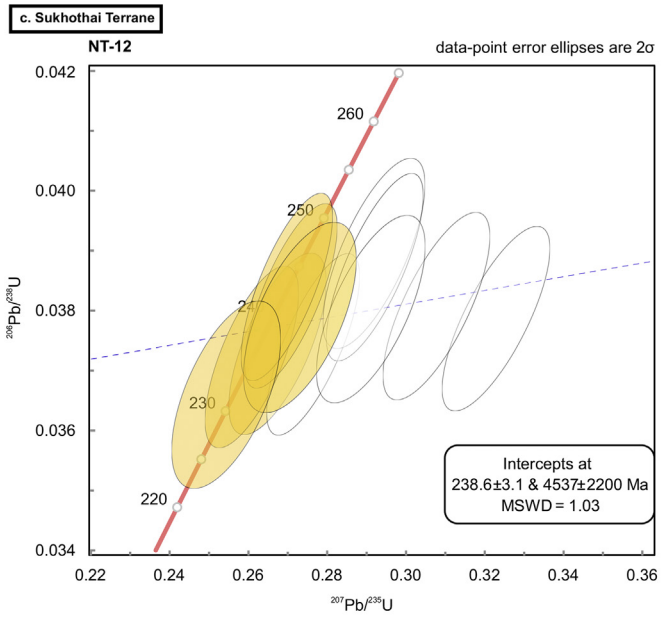

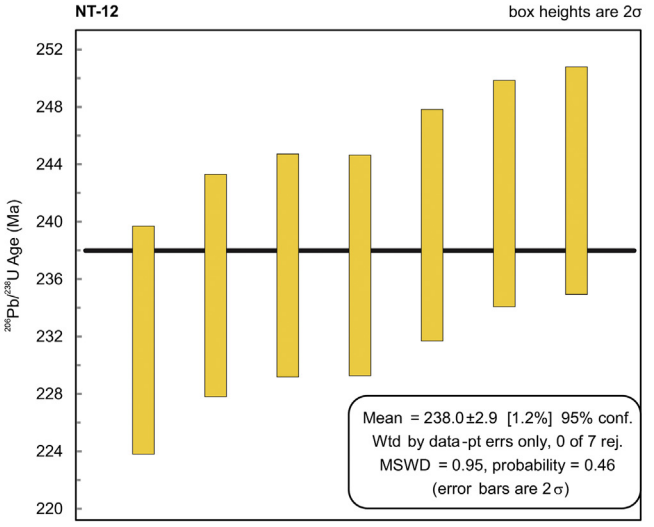

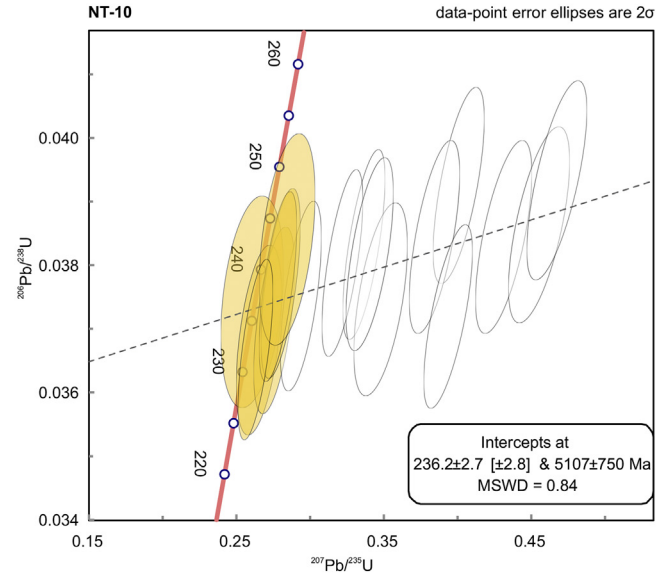

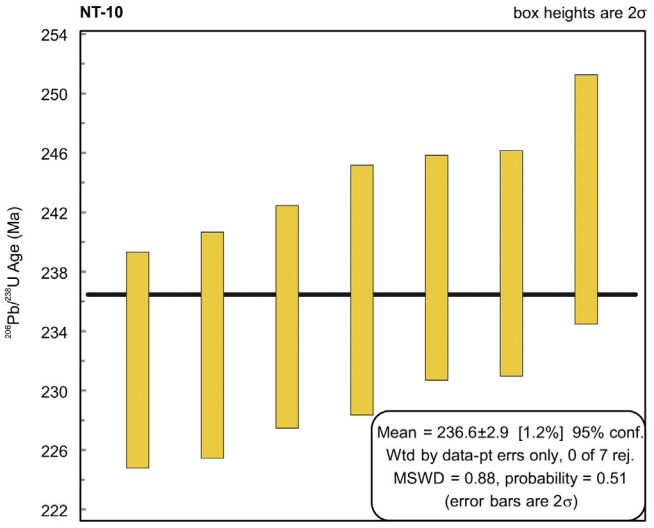

Fig. 3 *(continued)*.

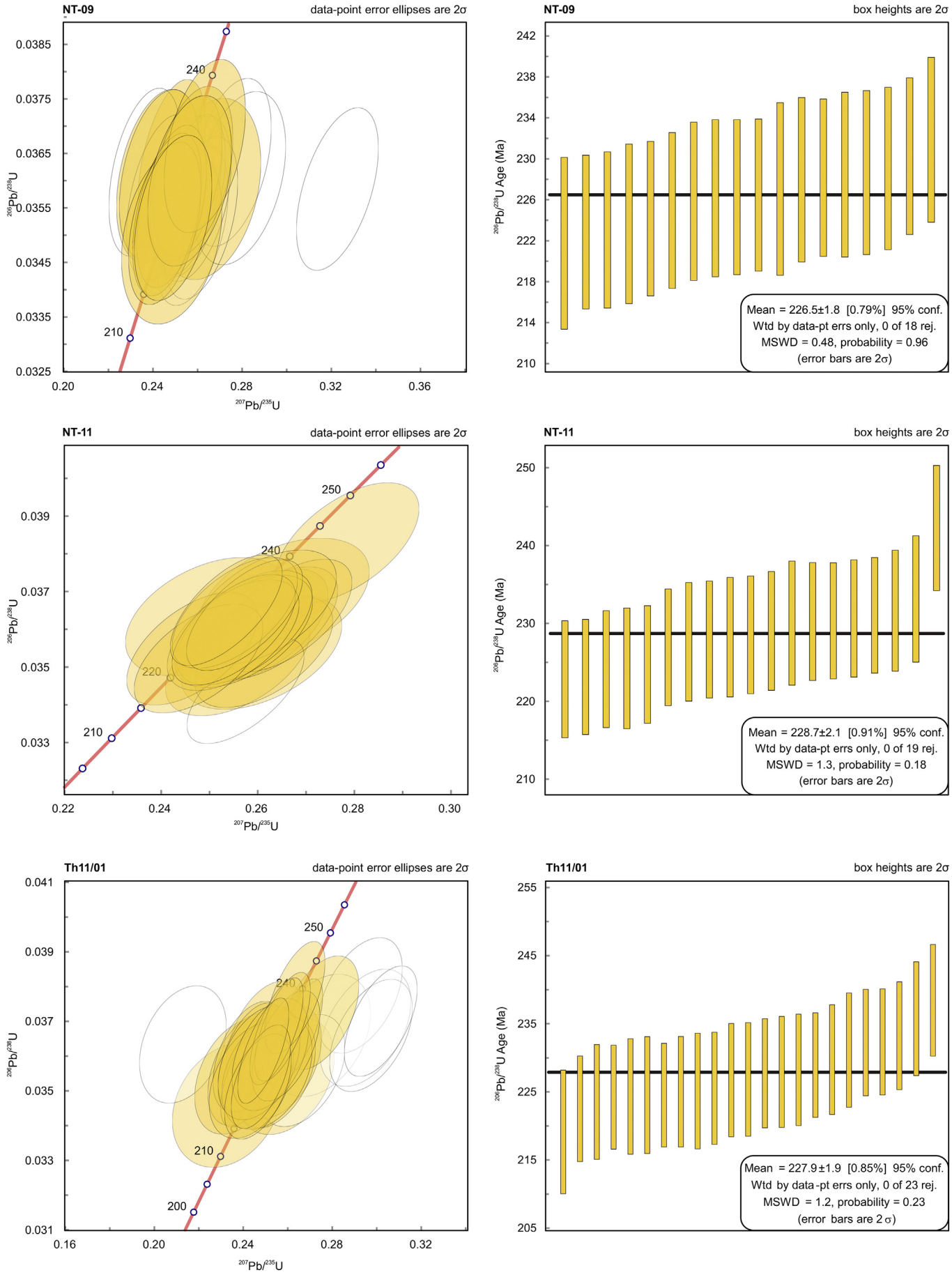

Fig. 3 *(continued)*.

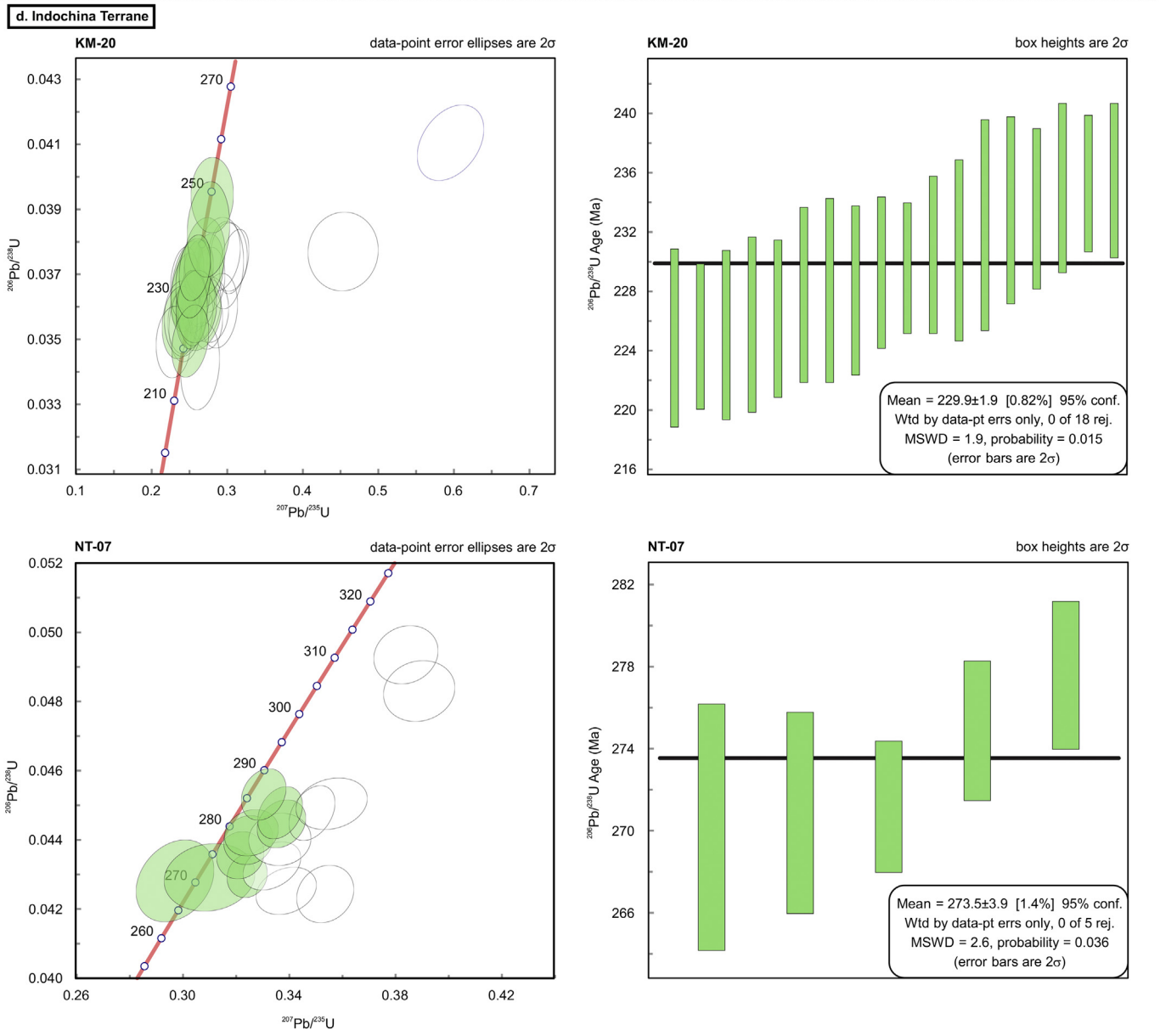

Fig. 3 *(continued)*.

is the interpreted crystallisation age of NT-07. NT-07 also included earliest Permian and latest Carboniferous ages that were interpreted as inherited analyses. This sample yielded a spread of analyses that may suggest limited post-crystallisation disturbance of the isotopic system that is supported by the sericitisation of feldspars seen in thin section (Dew et al. submitted, Fig. 1u, v).

3.2. Zircon Lu–Hf isotope analysis

The $^{176}Hf/^{177}Hf$ and $^{176}Lu/^{177}Hf$ isotopes were measured and used to interpret the isotopic differentiation of the mantle and crustal reservoirs (Patchett and Tatsumoto, 1980). They reflect the separation time of the parental magma from the mantle (Gardiner et al., 2016; Kemp et al., 2006). Hafnium data were plotted in epsilon Hf (εHf) versus age space, displayed in Fig. 4, to highlight the similarities and differences in crustal evolution of similar aged zircon grains (Kemp et al., 2006). For the interpreted magmatic ages, the U–Pb weighted average age was used to calculate $\varepsilon Hf_{(t)}$ where possible. For older inherited zircons, the individual U–Pb age for that analyses was used to calculate $\varepsilon Hf_{(t)}$ values.

3.2.1. Sibumasu Terrane

The analysis of magmatic zircons from ST-49A for hafnium yielded $\varepsilon Hf_{(t)}$ values between −14.42 and − 11.73 (Fig. 4). For ST-16, Hf analyses were conducted on one magmatic zircon ($\varepsilon Hf_{(t)}$ of − 4.82) and seven interpreted inherited zircons yielding $\varepsilon Hf_{(t)}$ values between − 27.12 and + 0.98 (Fig. 4). The Hf analyses were conducted on six interpreted inherited zircons for RDT15_076A yield $\varepsilon Hf_{(t)}$ values between − 6.69 and + 9.03 (Fig. 4).

3.2.2. Inthanon Zone

Magmatic $\varepsilon Hf_{(t)}$ values from RDT16_053 range between − 18.60 and − 10.49 (Fig. 4). The hafnium isotopic analyses of magmatic zircons from Th11/02 yielded $\varepsilon Hf_{(t)}$ values between − 19.58 and

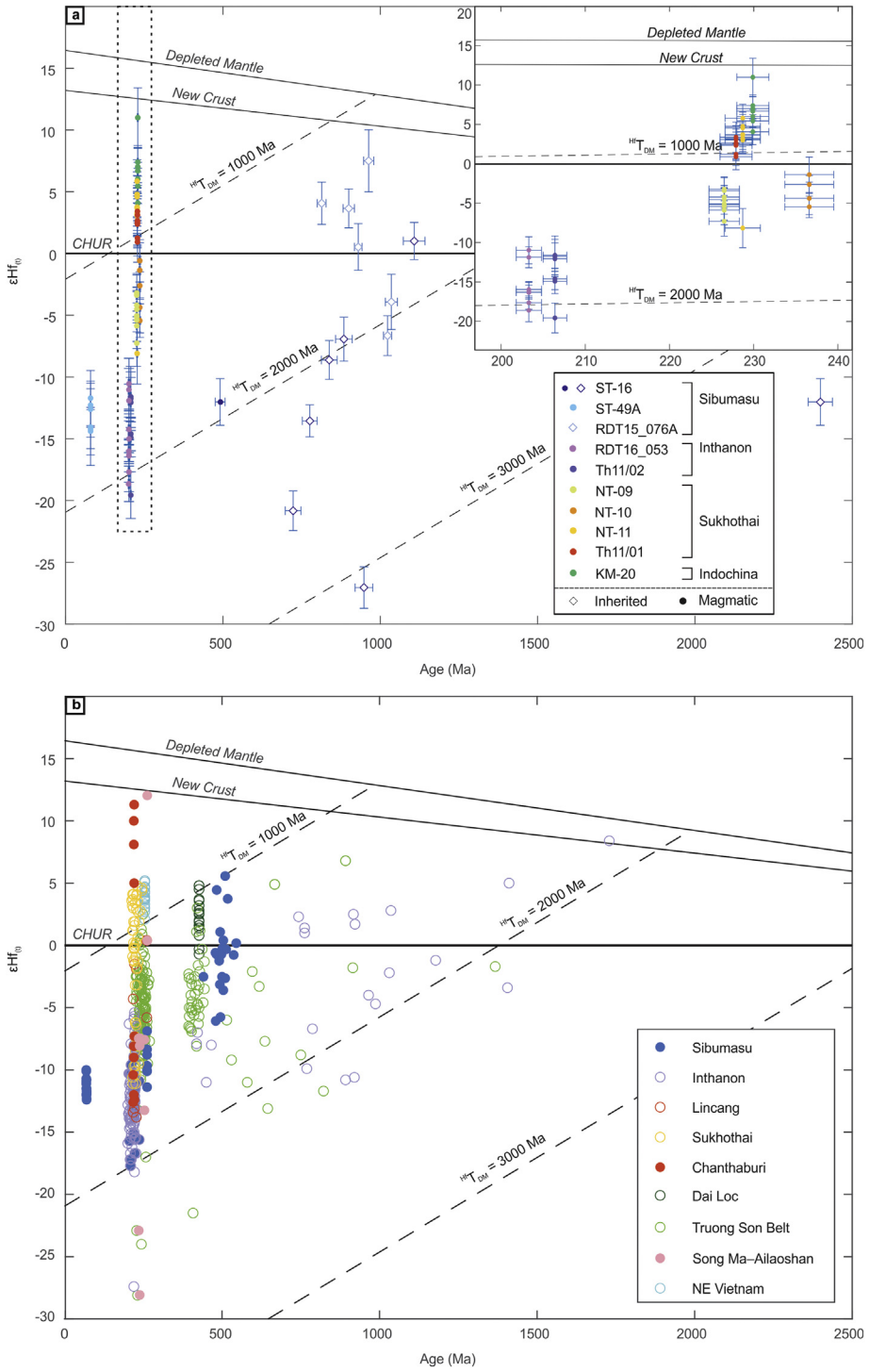

Fig. 4. a (top): Hafnium isotope diagram for the sampled granitoids, displayed as $\varepsilon Nd_{(t)}$ against the interpreted sample crystallisation age (the weighted average age). For interpreted inherited zircons, individual zircon spot U–Pb ages are used to calculate $\varepsilon Hf_{(t)}$. Both horizontal and vertical error bars show 2σ error. The dashed rectangle indicates the extent of the inset. The T_{DM} (crustal) Hf evolution lines are based on a $^{176}Lu/^{177}Hf$ ratio of 0.015 (Griffin et al. 2004). b (bottom): Hafnium isotope diagram for published granitoid data (see Dew et al., submitted for further details) displayed as $\varepsilon Nd_{(t)}$ against the age. The T_{DM} (crustal) Hf evolution lines are based on a $^{176}Lu/^{177}Hf$ ratio of 0.015 (Griffin et al. 2004).

− 11.62. The zircons from RDT16_053 and Th11/02 have a similar crystallisation age and yield a similar range of negative $\varepsilon Hf_{(t)}$ values.

3.2.3. Sukhothai Terrane

All Hf analyses from the Sukhothai Terrane were taken from magmatic zircons (Fig. 4). The analysis of nine zircons from NT-09 yielded $\varepsilon Hf_{(t)}$ values between − 7.31 and − 3.23. The hafnium analysis of five magmatic zircons from the NT-10 sample yielded $\varepsilon Hf_{(t)}$ values between − 5.47 and − 0.61 (Fig. 4). The hafnium analysis of seven magmatic zircons from the Th11/01 sample yielded $\varepsilon Hf_{(t)}$ values between + 0.89 and + 3.37. The analysis of nine zircons from NT-11 for hafnium yielded $\varepsilon Hf_{(t)}$ values between − 8.12 and + 5.85, but, eight of the zircons analysed contained positive $\varepsilon Hf_{(t)}$ values between + 3.00 and + 5.81, however, one magmatic zircon from this sample yielded a negative $\varepsilon Hf_{(t)}$ value of − 8.71.

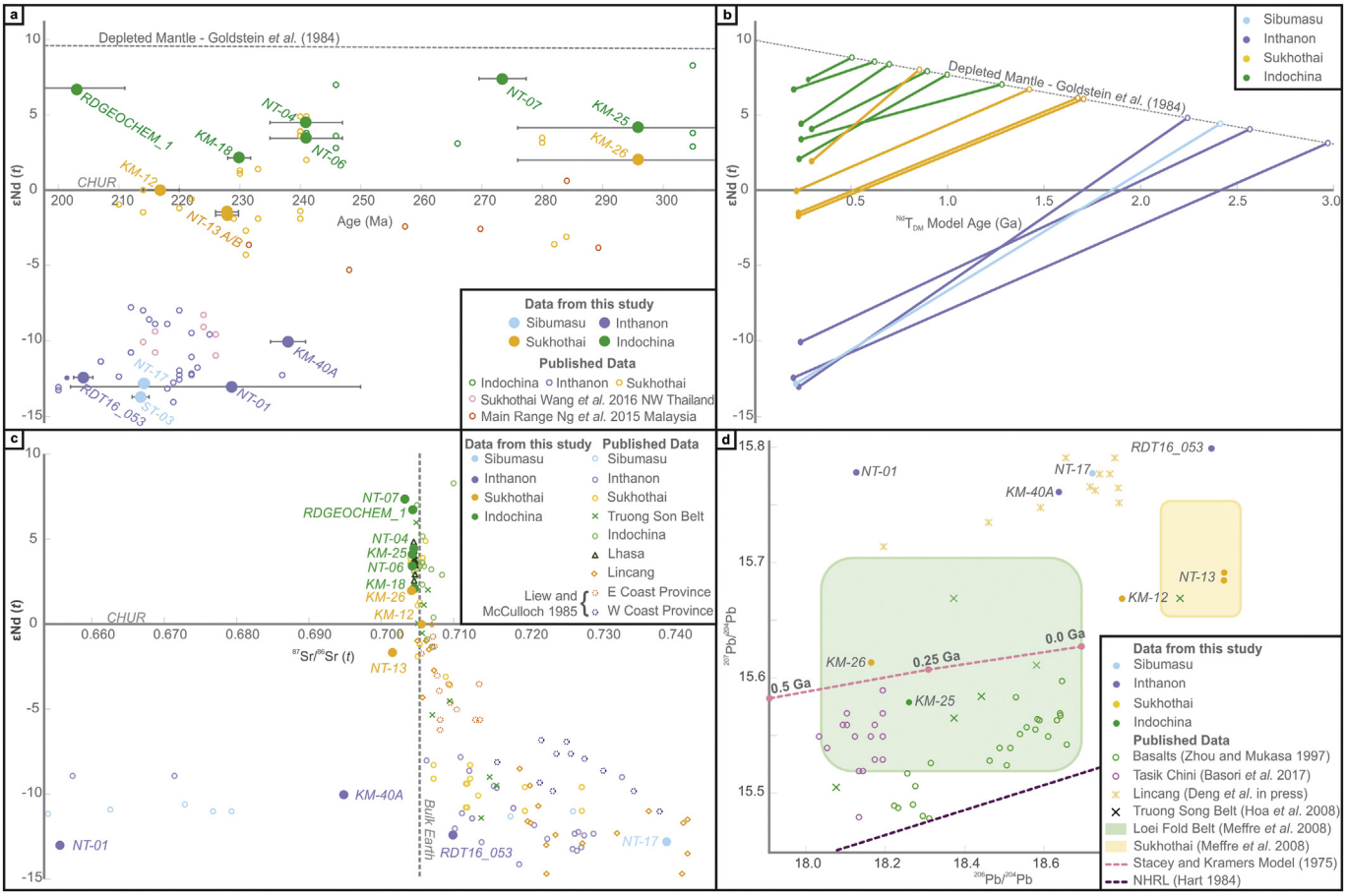

Fig. 5. a (top left): $\varepsilon Nd_{(t)}$ against age. Depleted Mantle assumes the linear depletion of the mantle as per (Goldstein et al., 1984). Error bars show age uncertainties, see Table 1 for references for ages used. b (top right): Plot of $\varepsilon Nd_{(t)}$ with depleted mantle model ages ($^{Nd}T_{DM}$) using assumed values from Goldstein et al. (1984). c (bottom left): $\varepsilon Nd_{(t)}$ against initial Sr. d (bottom right): Lead isotope ratio plot for granitoid analysed in this study with published Pb data. Reference lines from (Hart, 1984; Stacey and Kramers, 1975). References for published data tabulated in Dew et al., (submitted).

3.2.4. Indochina Terrane

Seven magmatic analyses from KM-20 yielded positive $\varepsilon Hf_{(t)}$ values ranging from + 4.06 to + 10.99 as shown in Fig. 4.

3.3. Sm—Nd, Sr and Pb whole-rock geochemistry

The whole-rock geochemistry of granitoid rocks from Thailand was used to infer the petrogenetic and tectonic history of the region. The Sm—Nd isotopic system was used, in a similar way to the Lu—Hf isotopic system in zircon, to interpret the isotopic differentiation of the mantle and crustal reservoirs. The Sm—Nd whole-rock technique is advantageous compared to the zircon Lu—Hf isotopic system since it can be used for zircon-poor lithologies and for smaller sample sizes. The Sm—Nd system was plotted firstly in Epsilon Nd (εNd) - age space shown in Fig. 5a, with interpreted depleted mantle model ages in Fig. 5b. Epsilon Nd ($\varepsilon Nd_{(t)}$) was also displayed with the initial $^{87}Sr/^{86}Sr$ ratios ($^{87}Sr/^{86}Sr_{(t)}$) in Fig. 5c to indicate the nature of the magmatic source for granitoids and assist in the discrimination of S- and I-type granitoids (Chappell and White, 1992, 2001; Ng et al., 2015a). Lead isotopes help establish the nature and origin of mixing components in the mantle due to the linear mixing relationship between the four Pb isotopes: the radiogenic ^{206}Pb, ^{207}Pb and ^{208}Pb and the non-radiogenic ^{204}Pb (Taylor et al., 2015). The ratios of $^{206}Pb/^{204}Pb$ and $^{207}Pb/^{204}Pb$ are displayed in Fig. 5d with the Stacey and Kramers (1975) terrestrial Pb evolution model and the Northern Hemisphere Reference Line (NHRL), outlined by Hart (1984), for comparison.

3.3.1. Sibumasu Terrane

The two samples from the Sibumasu terranes have negative $\varepsilon Nd_{(t)}$ values of −13.69 (ST-03) and − 12.80 (NT-17) as displayed in Fig. 5. These strongly negative $\varepsilon Nd_{(t)}$ values indicate the remelting of pre-existing continental crust. ST-03 contained anomalously low Nd concentrations (see Tables 6 and 7 of Dew et al. submitted), therefore we cannot be confident in the reliability of this value, although it is similar to the $\varepsilon Nd_{(t)}$ value found in the other Sibumasu sample, NT-17. The $^{87}Sr/^{86}Sr_{(t)}$ value of 0.739474 from NT-17 is an enriched upper continental crust signature (see Fig. 5c). In contrast, the $^{87}Sr/^{86}Sr_{(t)}$ value measured for ST-03 is highly anomalous at 1.476070, this may be due to the low Sr concentration of this sample at 23 ppm and its very high Rb/Sr ratio (Rb ppm is 904.4), which has been previously suggested by Romer et al. (2012) to create remarkably large uncertainties of the initial $^{87}Sr/^{86}Sr$ ratios. NT-17 is enriched in all three radiogenic Pb isotopes with ratios of $^{206}Pb/^{204}Pb$ 18.723486, $^{207}Pb/^{204}Pb$ 15.777563 and $^{208}Pb/^{204}Pb$ 38.819131 (Fig. 5d). The enriched radiogenic Pb isotopes measured in this sample suggests the involvement of recycled continental material.

3.3.2. Inthanon Zone

All three samples from the Inthanon Zone have strongly negative $\varepsilon Nd_{(t)}$ values (RDT16_053–12.40, KM-40A −10.04 and NT-01 − 13.01) indicating remelting of pre-existing continental crust (Fig. 5). The $\varepsilon Nd_{(t)}$ value of RDT16_053 of −12.40 is within the range of the $\varepsilon Hf_{(t)}$ values found from the zircons within this sample ($\varepsilon Hf_{(t)}$ between −18.60 to −10.49; Fig. 4). The Permo-Triassic $\varepsilon Hf_{(t)}$ values

found within the zircons from Sibumasu and Inthanon samples also display strong negative values. Similarly, negative $\varepsilon Nd_{(t)}$ values were also calculated for the two samples from the Sibumasu Terrane (Fig. 5a). The $^{87}Sr/^{86}Sr_{(t)}$ values for the Inthanon Zone have a wide variance from 0.655385 and 0.704255 (Fig. 5c). It is unreasonable for the initial $^{87}Sr/^{86}Sr$ ratios to be lower than values of Basaltic Achondrite Best Initial (0.69897 ± 0.00003). The anomalously low $^{87}Sr/^{86}Sr_{(t)}$ value from NT-01 of 0.655385 could be a result of a post-crystallisation shift in the Rb/Sr (high Rb 753.8 ppm and low Sr 52 ppm). The $^{87}Sr/^{86}Sr_{(t)}$ for KM-40A (0.694704) could have also experienced minor resetting within the Rb−Sr system. The enriched $^{87}Sr/^{86}Sr_{(t)}$ value of 0.704255 for RDT16_053 suggests a lower crustal source for this granitoid. The initial Pb ratios for RDT16_053 were $^{206}Pb/^{204}Pb$ 19.026140, $^{207}Pb/^{204}Pb$ 15.799454 and $^{208}Pb/^{204}Pb$ 39.397697. The Pb ratios for KM-40A were $^{206}Pb/^{204}Pb$ 18.642169, $^{207}Pb/^{204}Pb$ 15.762181 and $^{208}Pb/^{204}Pb$ 38.999662. The Pb ratios for NT-01 were $^{206}Pb/^{204}Pb$ 18.127639, $^{207}Pb/^{204}Pb$ 15.778859 and $^{208}Pb/^{204}Pb$ 35.393159. The enriched radiogenic Pb isotopes measured in these sample suggests that it was sourced from continental material that has experienced multiple recycling events. NT-17, the only sample for Pb isotopic analyses from the Sibumasu Terrane, is within the isotopic range of the samples from Inthanon (Fig. 5d).

3.3.3. Sukhothai Terrane

The duplicate runs of NT-13 contained similar $\varepsilon Nd_{(t)}$ values of −1.66 and − 1.45. The older KM-26 sample from further north also located in the Sukhothai Terrane was more juvenile in nature with an $\varepsilon Nd_{(t)}$ value of +1.97. KM-12, located further south gave a $\varepsilon Nd_{(t)}$ value of −0.00. These four $\varepsilon Nd_{(t)}$ values from Sukhothai sit very close to the CHUR line (Fig. 5a). The Sukhothai samples gave $^{87}Sr/^{86}Sr_{(t)}$ values of 0.701347 (NT-13), 0.705499 (KM-12) and 0.704083 (KM-26). Although the $^{87}Sr/^{86}Sr_{(t)}$ data sit within the bulk Earth range, $\varepsilon Nd_{(t)}$ values are slightly enriched compared to the observable silicate Earth (Fig. 5c). These results indicate a relatively undepleted mantle source or a depleted mantle source, which has been contaminated by crustal material with an enriched isotopic signature. These data, like the $\varepsilon Hf_{(t)}$ results (Fig. 4), support a hypothesis where the Sukhothai arc was built on older continental material (Hara et al., 2017). The duplicate runs of NT-13 gave Pb ratios of $^{206}Pb/^{204}Pb$ 19.057330 (A) and 19.058107 (B), $^{207}Pb/^{204}Pb$ 15.685211(A) and 15.691958 (B) and $^{208}Pb/^{204}Pb$ 38.608086 (A) and 38.624095 (B). The Pb ratios for KM-26 ($^{206}Pb/^{204}Pb$ 18.168563, $^{207}Pb/^{204}Pb$ 15.614036 and $^{208}Pb/^{204}Pb$ 36.9956861) are very close to the Stacey and Kramers (1975) terrestrial lead evolution model (see Fig. 5d). The Pb ratios of KM-12 are $^{206}Pb/^{204}Pb$ 18.801927, $^{207}Pb/^{204}Pb$ 15.669479 and $^{208}Pb/^{204}Pb$ 38.391281 are slightly enriched in radiogenic lead. Overall the Pb isotopes from the Sukhothai Terrane closely follow the Stacey and Kramers (1975) terrestrial lead evolution model, although KM-12 and NT-13 are slightly more enriched in radiogenic Pb. The whole-rock data from this study are within the range of the published data from the Sukhothai Terrane, although KM-26 appears to have more isotopic affinity to the Indochina Terrane (see Fig. 5).

3.3.4. Indochina Terrane

All $\varepsilon Nd_{(t)}$ values from the six samples from the Indochina Terrane are positive, ranging between +2.11 to +7.40, reflecting juvenile sources, with minimal continental crust involvement. The samples from the Indochina Terrane have $^{87}Sr/^{86}Sr_{(t)}$ values ranging from 0.703140 to 0.704491. These values are within the range expected for primitive bulk Earth. The Pb ppm concentration within all samples from Indochina besides KM-25, were below the 1 ppm detection limit of the XRF, therefore, whole-rock TIMS analyses were not completed on these samples. The Pb ratios for KM-25 were $^{206}Pb/^{204}Pb$ 18.263816, $^{207}Pb/^{204}Pb$ 15.579570 and $^{208}Pb/^{204}Pb$ 37.462045. This plots in $^{206}Pb/^{204}Pb$, $^{207}Pb/^{204}Pb$ space between the crustal evolution model and the MORB-like reservoir of the NHRL (see Fig. 5d; Hart, 1984; Stacey and Kramers, 1975).

4. Timing of magmatism for Thailand's granitoids

In this study, latest Triassic magmatism is observed only in samples from the Sibumasu Terrane and the Inthanon Zone (see Fig. 3). These ages are consistent with published data from Sibumasu and Inthanon with ages spanning 240–200 Ma (Ahrendt et al., 1993; Charusiri et al., 1993; Gardiner et al., 2016; Kawakami et al., 2014; Ng et al., 2015a; Searle et al., 2012; Wang et al., 2016c). These are thought to be supra-subduction zone granitoids, forming coeval with the closure of the Palaeo-Tethys Ocean (i.e. the older granites from the Sukhothai Terrane) and the subsequent collision of Sibumasu with the Sukhothai and Indochina terranes during the Upper Triassic (Searle et al., 2012).

Unlike the exclusively Permo-Triassic crystallisation ages found in this study from Indochina and Sukhothai, the Sibumasu and Inthanon granitoids contained concordant data of other ages. The weighted average age from ST-16 and inherited zircons from samples in the Sibumasu and Inthanon regions are Cambrian in age (see Fig. 3). Cambrian-aged crystalline basement has been found previously in the Sibumasu Terrane and was associated with arc-related magmatism along the Gondwanan Indo-Australian margin (Lin et al., 2013). Cretaceous crystallisation ages found in samples from Sibumasu and Inthanon are also represented in published data from these terranes and are synchronous with the closure of the Neo-Tethys Ocean (Jiang et al., 2017; Kanjanapayont et al., 2012; Metcalfe, 2013). U−Pb data from samples ST-16 and ST-13 suggest limited isotopic disturbance at this time, consistent with a thermal overprint in this terrane at this time. Additionally the samples from Sibumasu and Inthanon contain abundant Precambrian inherited zircon grains (3200–600 Ma, see Fig. 3), studies such as Wang et al. (2016c) have also found inherited zircon grains ranging from 2545 to 400 Ma.

In this study, only early Ladinian (final stage of the Middle Triassic) crystallisation ages are found in the samples from the Sukhothai Terrane (see Fig. 3). Magmatic ages ranging from 296 to 200 Ma are found in the Sukhothai Terrane (This study; Beckinsale et al., 1979; Charusiri et al., 1993; Cobbing, 2011; Hansen and Wemmer, 2011; Meffre et al., 2008; Ng et al., 2015b; Qian et al., 2017; Singharajwarapan and Berry, 2000; Sone et al., 2012; Wang et al., 2016c; Zaw et al., 2014). The ages from the Indochina Terrane express prolonged Permo-Triassic magmatism compared to the later Triassic ages seen in the samples from the Inthanon Zone and Sibumasu Terrane (see Figs. 3 and 5). Published data from the Indochina Terrane are consistent with this study's dataset and indicate ages spanning from 310 to 203 Ma (Arboit et al., 2016; Charusiri et al., 1993; Halpin et al., 2016; Kamvong et al., 2014; Ng et al., 2015b; Salam et al., 2014; Zaw et al., 2014). The Ladinian (late Middle Triassic) ages found in the Sukhothai and Indochina granitoids are likely to be as a result of the early stages of the South China and Cathaysia collision with Vietnam and Indochina (Halpin et al., 2016; Lepvrier et al., 2004), or the similarly timed collision between Indochina and Sukhothai (Morley et al., 2013).

5. Isotopic characteristics of Thailand

The data collected in this study shows that the three main terranes in Thailand (Sibumasu, Sukhothai and Indochina) that show distinctions in their basement isotopic characteristics (see Figs. 4 and 5).

5.1. Sibumasu and Inthanon Terranes

The Sibumasu and Inthanon terranes exhibit similar age patterns and isotopic characteristics, suggesting a similar history. Both terranes generally contain evolved recycled crust, which is a consistent feature of the Hf, Sm−Nd, Sr and Pb isotopic signatures of the Cambrian–Cretaceous samples from this region (see Figs. 4 and 5). The inherited zircon

domains from the Sibumasu samples also have evolved signatures, seen in the negative $\varepsilon Hf_{(t)}$ values for ages ranging from 2400 to 600 Ma, providing further evidence for multiple recycling events (Fig. 4). The elevated $^{207}Pb/^{204}Pb$ ratios measured in the samples from the Sibumasu Terrane and the Inthanon Zone suggest the involvement of recycled continental material in these terranes (Taylor et al., 2015). Evolved isotopic signatures are also evident in published Sibumasu and Inthanon studies from Thailand, Malaysia and Myanmar (see Figs. 4–5; Gardiner et al., 2016; Jiang et al., 2017; Kanjanapayont et al., 2012; Lin et al., 2013; Ng et al., 2015a; Wang et al., 2016a).

A wide range of $\varepsilon Hf_{(t)}$ signatures are observed in the older inherited grains from RDT15_076A and ST-16 from Sibumasu (see Fig. 4). This is consistent with the isotopic signatures of S-type granitoids that can have more heterogeneous source material (Chappell and White, 2001; Cobbing et al., 1992). The granitoids from Inthanon and Sibumasu have been previously identified to have peraluminous S-type characteristics indicating that their source rocks had been through an earlier sedimentary cycle (Charusiri et al., 1993; Cobbing et al., 1992; Liew and McCulloch, 1985; Qian et al., 2017; Searle et al., 2012; Yokart et al., 2003). Petrographic investigations confirmed the peraluminous characteristics of ST-16 in which we found the disintegration of garnet crystals, typical for S-type granitoids (see Fig. 1 of Dew et al. (submitted)).

Granites from the Sibumasu Terrane have been previously interpreted to be syn-collisional granitoids formed during the final stages of the Permo-Triassic Indosinian Orogeny and the closure of the Palaeo-Tethys Ocean (Beckinsale et al., 1979; Bunopas, 1981; Charusiri et al., 1993; Cobbing et al., 1992; Metcalfe, 2013; Pour et al., 2017; Searle et al., 2012; Yokart et al., 2003). The crustal thickening and melting of the Sibumasu Terrane during the Indosinian Orogeny is a possible mechanism for the formation of these S-type granitoids seen both in the Sibumasu Terrane and the Inthanon Zone (Bunopas, 1981; Charusiri et al., 1993; Mitchell, 1992; Searle et al., 2012).

Granites from the Sibumasu Terrane have been previously interpreted to be syn-collisional granitoids formed during the final stages of the Permo-Triassic Indosinian Orogeny and the closure of the Palaeo-Tethys Ocean (Beckinsale et al., 1979; Bunopas, 1981; Charusiri et al., 1993; Cobbing et al., 1992; Metcalfe, 2013; Pour et al., 2017; Searle et al., 2012; Yokart et al., 2003). The crustal thickening and melting of the Sibumasu Terrane during the Indosinian Orogeny is a possible mechanism for the formation of these S-type granitoids seen both in the Sibumasu Terrane and the Inthanon Zone (Bunopas, 1981; Charusiri et al., 1993; Mitchell, 1992; Searle et al., 2012).

5.2. Sukhothai Terrane

The isotopic values from the Sukhothai samples in this study are similar to values expected for the bulk silicate Earth or undifferentiated chondrite models (see Figs. 4 and 5). Similar isotopic values have been found in previous studies (e.g. Barr et al., 2006; Du et al., 2016; Ng et al., 2015b; Qian et al., 2017). In this study, the granitoids from the Sukhothai Terrane form a continuum from more juvenile metaluminous I-type granitoids in the east through to more crustally evolved granitoids in the west. These data are within the range found in previous studies from Sukhothai and its equivalent terranes (Cobbing, 2011; Mahawat et al., 1990; Qian et al., 2017; Singharajwarapan and Berry, 2000). The petrogenesis causing these characteristics has been previously attributed to a hybridised source of a juvenile mafic magma with an ancient meta-sedimentary component (Ng et al., 2015b; Qian et al., 2017; Wang et al., 2016c). Further evidence for this origin is from a detrital study by Hara et al. (2017), which concluded that the Sukhothai arc system was built on older continental material.

5.3. Indochina Terrane

Data from the Thailand sector of the Indochina Terrane are predominantly from its western margin due to thick sedimentary cover in the Khorat Plateau further east. The combination of data from this study with isotopic data from published works indicates that the Thai part of the Indochina Terrane is relatively juvenile (Fig. 5; Arboit et al., 2016; Intasopa and Dunn, 1994; Kamvong et al., 2014; Qian et al., 2016; Wang et al., 2016b). The granitoids from the Indochina Terrane are metaluminous with an I-type affinity (See Fig. 5; Charusiri et al., 1993; Salam et al., 2014). Kamvong et al. (2014) found adakites in the Loei and Truong Son Belts suggesting their petrogenesis from mantle-modified slab melts. Similarly, Salam et al. (2014) suggests arc-derived magma origins produced by the interaction between the depleted mantle wedge and subduction-derived melts and fluids. There are few available data on the granitoids within the Cambodian sector of the Indochina Terrane. However, one study based on magnetic susceptibility and major and trace elements by Kong et al. (2012) implies that I-type granitoids are also found in this southeastern domain of the Indochina Terrane.

5.4. Spatial distribution of the isotopic signatures in Thailand and neighbouring regions

Vervoort et al. (1999) used Archean to recent samples from a wide range of depositional environments to demonstrate the behaviour of Lu—Hf and Sm—Nd isotopic systems in the global sedimentary system. The crustal array define this isotopic relationship as $\varepsilon Hf = 1.34\varepsilon Nd + 2.82$ (Vervoort et al. 1999). For this study, all the available published $\varepsilon Nd_{(t)}$ and recalculated $\varepsilon Hf_{(t)}$ data from Thailand and neighbouring regions of Myanmar, Laos, China and Vietnam were used to create an $\varepsilon Nd_{(t)}$ grid, to be used as a visualisation tool to highlight any trends in the isotopic characteristics.

The $\varepsilon Nd_{(t)}$ model was generated using the "natural neighbor" analyst tool in ArcGIS, to place the data into a spatial context. The grid was then clipped to the coastline and manually buffered around the outermost data points. The resultant model is shown in Fig. 6. Although in some regions the density of the $\varepsilon Nd_{(t)}$ and recalculated $\varepsilon Hf_{(t)}$ data is relatively low and no external constraints were used, the interpolation model highlights the different terranes and their boundaries. It also emphasises faults and major sutures, including the Three Pagodas Fault, the Klaeng Tectonic Line in SE Thailand and the complex Mae Ping Fault system including the Chainat Duplex and splays further east (see Fig. 6).

From this grid, a definable eastwards trend towards increasing juvenile characteristics occurs in Thailand (Fig. 6). The data in Fig. 6 clearly differentiates the juvenile nature of the Indochina Terrane from the more evolved Sibumasu and Inthanon. Additionally, the grid accentuates the isotopic difference between juvenile western Indochina to the more evolved Truong Son Belt of northwest Vietnam near the boundary zone between Indochina and South China (Liu et al., 2012; Wang et al., 2016b).

Fig. 6 also illustrates that the Sukhothai Terrane is less juvenile than the Indochina Terrane. The mixed isotopic characteristics of the Sukhothai Terrane require a relatively undepleted mantle source or a depleted mantle source that has been contaminated with old crust carrying an enriched isotopic signature. From this study's isotopic data and previously published studies, the most likely explanation is that a juvenile magma was mixed with evolved crustal material to produce the Sukhothai granitoids. The spatial position of the Sukhothai Terrane between the juvenile Indochina Terrane and the evolved Sibumasu Terrane and the trend of increasing juvenility eastwards through the Sukhothai Terrane implies that Sukhothai was a juvenile arc derived from Indochina, but incorporated evolved continental crust, similar to the Sibumasu Terrane, prior to or during granitoid emplacement.

5.5. Model ages for Thailand's basement

Barovich and Patchett (1992) demonstrated the overall insensitivity of the Nd and Hf isotopic systems in granitoids to extreme deformational events, lending confidence to the use of Nd and Hf isotopic

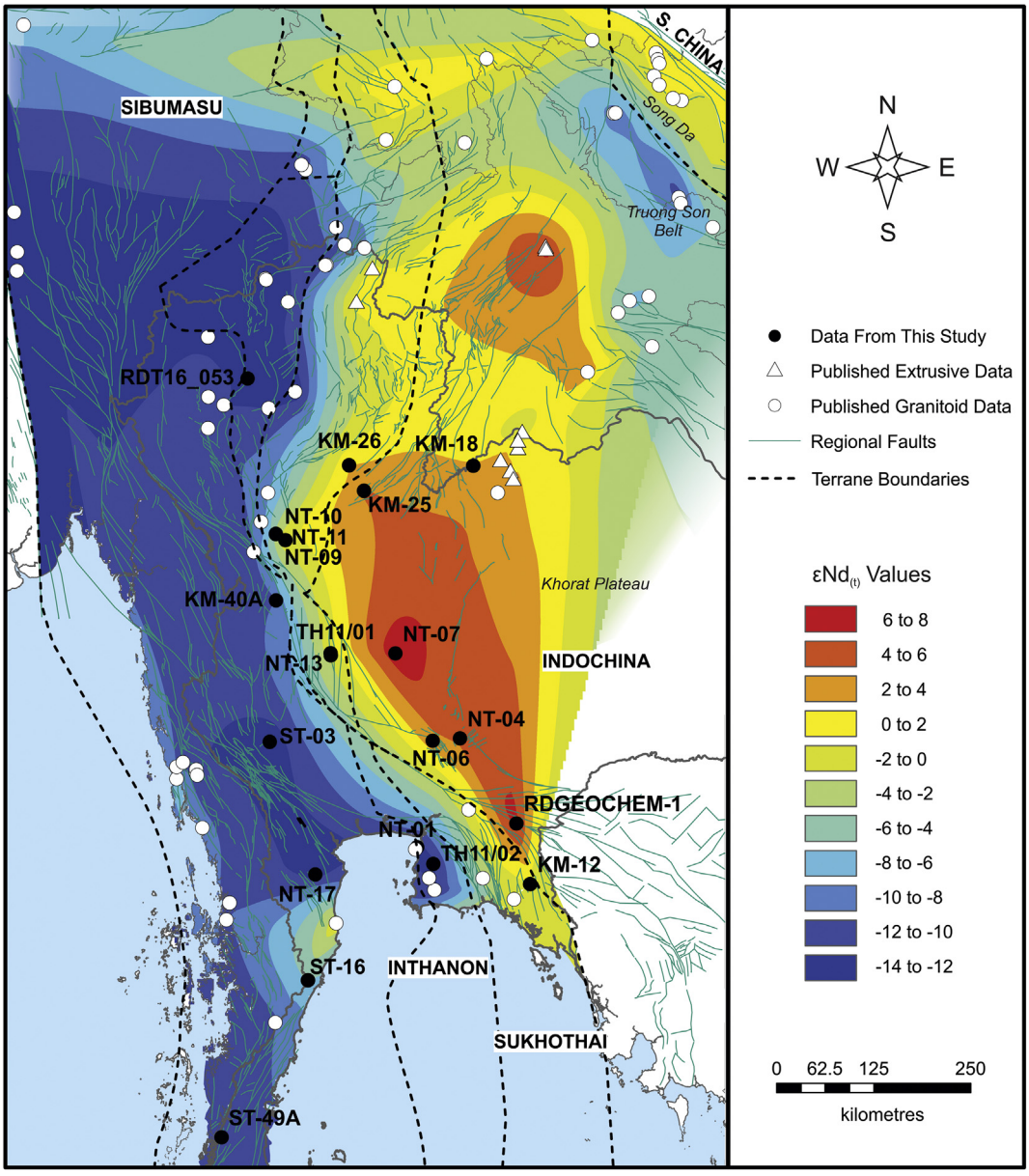

Fig. 6. A map collating all available $\varepsilon Nd_{(t)}$and $\varepsilon Hf_{(t)}$ data from Thailand and neighbouring regions, references for published data tabulated in Dew et al., (submitted).The data have been scaled by colour and gridded in ArcGIS using the "natural neighbor" analyst tool, to assist in visualising the data in a spatial context.Data clearly differentiates the juvenile Indochina Terrane from the other more evolved terranes, showing a trend of increasing juvenility to the east in Thailand, with the dark blue highly negative $\varepsilon Nd_{(t)}$ values in the Sibumasu Terrane moving eastwards into the orange to red positive $\varepsilon Nd_{(t)}$ values in the more juvenile Indochina Terrane.

systems, and hence model ages, in crustal evolution studies. Hafnium crustal depleted mantle model ages ($^{Hf}T_{DM}$, shown in Fig. 4) denote a minimum formation age for the source material of the zircon's parental magma (Gardiner et al., 2016; Kemp et al., 2006; Sevastjanova et al., 2011). These model ages were calculated for each zircon assuming the zircon grain growth reservoir was average continental crust with $^{176}Lu/^{177}Hf$ values of 0.0015 (Griffin et al., 2002). The Nd depleted mantle model ages ($^{Nd}T_{DM}$, shown in Fig. 5b) similarly reflect the time of the differentiation of the crust from the mantle but is a representation for the whole rock rather than individual zircons. However, since $^{Nd}T_{DM}$ samples the whole rock, if it is inhomogeneous in age and the material has been extracted from the mantle at various times, then the model age then represents an "average continental crustal residence time" (Arndt and Goldstein, 1987). Together, these model ages, when supported by other geological constraints i.e. zircon U—Pb inheritance, can be used to infer the rock's journey from the mantle to crust (Arndt and Goldstein, 1987; Gao et al., 2017; McCulloch, 1987).

5.5.1. Sibumasu Terrane

The depleted mantle model ages (T_{DM}) from the magmatic zircon Hf analyses in this study range between 2.02 Ga to 1.73 Ga with an average of 1.92 Ga. One Sm—Nd model age (T_{DM}) was calculated from the Sibumasu Terrane (NT-17) yielding an age of 2.41 Ga. This range of older heterogeneous T_{DM} values observed in the Sibumasu granitoids suggests that these granitoids were formed by assimilating or remelting older crustal material, which is consistent with the isotopic signatures analysed in this study. The $^{Hf}T_{DM}$ model ages found in this study are consistent with zircon inheritance found in this study (Figs. 2 and 3) and other published studies from the Sibumasu Terrane (Gardiner et al., 2016; Jiang et al., 2017; Liew and McCulloch, 1985; Lin et al., 2013; Sevastjanova et al., 2011). Although the older Sm—Nd model age from

this study is in agreement with the zircon inheritance ages (see Figs. 2, 3, 4 and 5), this age is not commonly reported in the literature. A minor model age peak of 2.8–2.5 Ga was mentioned in Sevastjanova et al. (2011).

5.5.2. Inthanon Zone

The corresponding $^{Hf}T_{DM}$ model ages from the magmatic $\varepsilon Hf_{(t)}$ data in this study are between 2.44 Ga and 1.87 Ga (Fig. 4). The $^{Nd}T_{DM}$ from this study range between 2.97 Ga to 2.24 Ga with an average of 2.60 Ga. The U—Pb zircon inheritance ages are consistent with these model ages (Fig. 3). These values suggest that these granitoids were produced by assimilating or remelting 2.44–1.87 Ga crustal material. These model ages correspond to values for other rocks in the Sibumasu and Inthanon terranes along with their equivalents throughout Asia (Hansen and Wemmer, 2011; Qian et al., 2017; Sevastjanova et al., 2011; Wang et al., 2016c).

5.5.3. Sukhothai Terrane

The solely magmatic data from the Sukhothai Terrane yielded Lu—Hf model ages between 1.74 and 0.86 Ga, with an average of 1.27 Ga. The Sm—Nd model ages were within a similar age range (1.71 to 0.85 Ga with an average of 1.42 Ga). The $^{Nd}T_{DM}$ from KM-26, close to the Indochina Terrane (0.85 Ga), affects the range of model ages seen in the Sukhothai Terrane since this value is 570 Ma younger than the next youngest model age from this terrane. This age is more comparable with model ages found in Indochina. The T_{DM} ages for the Sukhothai samples in this study are within the range of previously published T_{DM} values (1.95 to 0.96 Ga, with peaks at 1.90 Ga and 1.10 Ga) from northwest Thailand (Wang et al., 2016c).

5.5.4. Indochina Terrane

The corresponding T_{DM} model ages from the Nd data are between 1.28 and 0.50 Ga with an average of 0.83 Ga (Fig. 4). One sample from the Indochina Terrane was used for zircon Hf analyses (KM-20), giving corresponding $^{Hf}T_{DM}$ model ages between 0.97 and 0.53 Ga. These values suggest that the source material is largely juvenile, with minimal crustal input. Similar model ages have been published from the Khao Khwang Fold-Thrust Belt of Indochina's western margin (location is shown in Fig. 1a; Arboit et al., 2016). Previous studies have highlighted that there is little evidence of the existence of the western Thai sector of the Indochina Terrane prior to the middle Silurian (Cocks and Torsvik, 2013; Ridd, 2011). However, published detrital zircon studies from the Indochina Terrane suggest that the protoliths of the metasedimentary basement rock formed during the Neoproterozoic–early Paleozoic (Burrett et al., 2014). The model ages calculated for the Indochina Terrane in this study are much younger than the previous published source estimates from equivalent regions in Vietnam and Malaysia of >3.7 Ga to 1.88 Ga (Sevastjanova et al., 2011; Usuki et al., 2013).

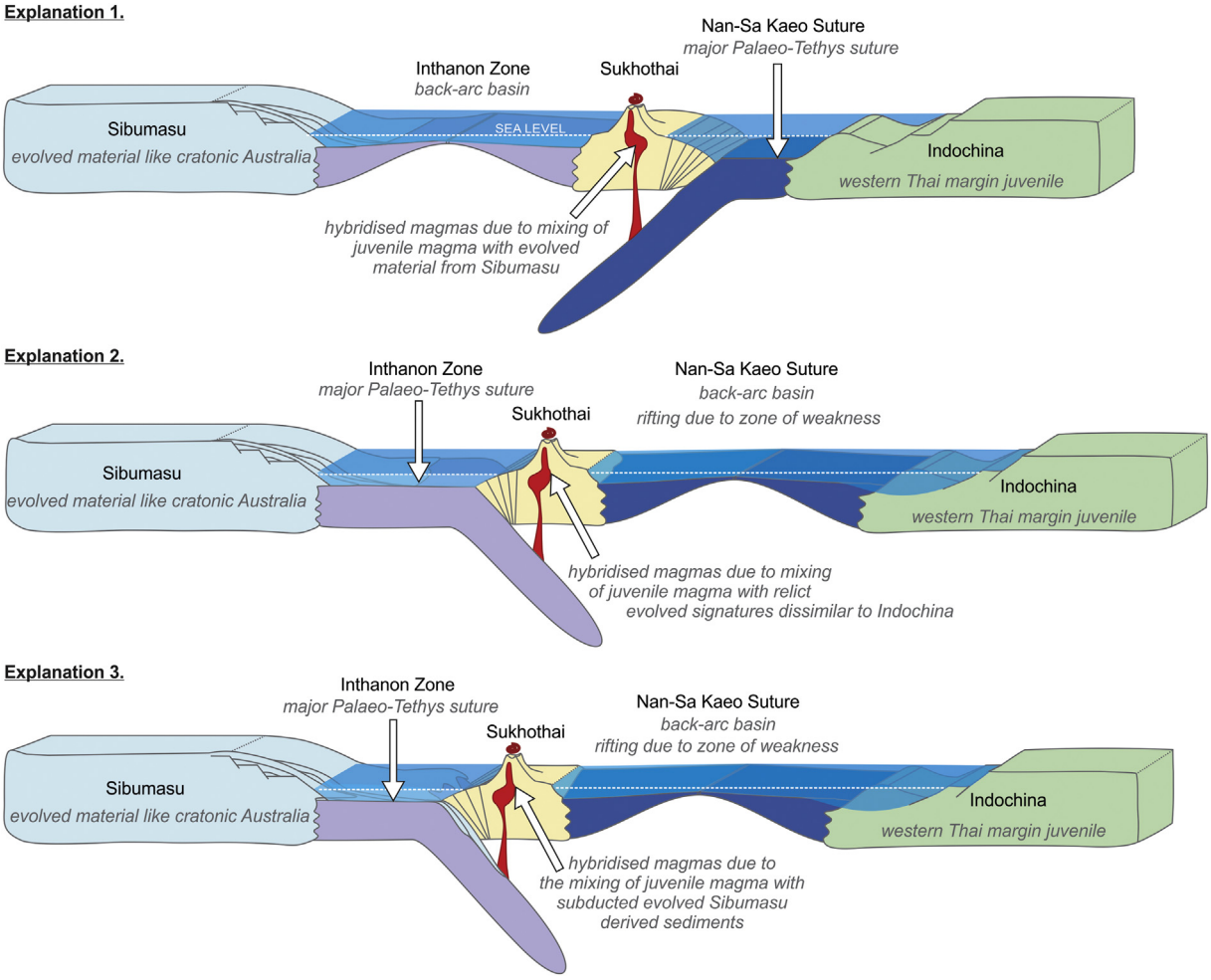

Fig. 7. Diagrams for the potential tectonic development of the Thai terranes.a: Explanation 1) The Sukhothai arc would have sat outboard of Sibumasu on the northwest Australian margin of Gondwana.In this model, the Inthanon Zone would represent the back-arc basin between Sibumasu and Sukhothai and the main Palaeo-Tethys suture separates Sukhothai and Indochina (the Nan Suture).b. Explanation 2) The Sukhothai arc was derived from Indochina, but contains relict Precambrian signatures.This would require a zone of weakness between the more juvenile western Thai Indochina Terrane and the evolved Sukhothai Terrane crust to have been exploited by the back-arc extension that separated these terranes.c. Explanation 3) The hybridised nature of the mid-Triassic granitoids in the Sukhothai Terrane may be due to the incorporation of evolved distal passive margin sequences of the Sibumasu Terrane as they approached the subduction zone.

6. Implications for terrane evolution

This study indicates that western Indochina is relatively juvenile with middle Mesoproterozoic to Cambrian $^{Nd}T_{DM}$ model ages. Regions that conceivably have similar-aged material to the Indochina Terrane are the west coast of Australia (Collins, 2003), and northeast margin of India (Ghosh et al., 2005), both are locations where the Pinjarra Orogen crops out. The Neoproterozoic–Cambrian Pinjarra Orogen forms part of a much larger orogenic belt that can be traced along Western Australia and through eastern Antarctica (Burrett et al., 2014; Collins, 2003; Ghosh et al., 2005). Published $^{Nd}T_{DM}$ ages of 1.18 to 1.08 Ga from southwestern Australia are consistent with the older Mesoproterozoic model ages for the Indochina Terrane in this study (Fletcher and Libby, 1993; McCulloch, 1987; Wilde, 1999). Other possible neighbouring domains could be northwest India (Wang et al., 2017), along with other localities where the East African Orogen intersects the northern Gondwanan margin i.e. the Arabian Nubian Shield (Blades et al., 2015).

Previous detrital zircon work on Paleozoic—Mesozoic sediments demonstrates that the Thai parts of the Indochina Terrane had U—Pb and Lu—Hf affinities to the rest of Indochina (including Central Vietnam and the Truong Son Belt), South China, Qiangtang and Lhasa terranes during the early Paleozoic (Burrett et al., 2014; Usuki et al., 2013). Published granitoid geochemistry from the Lhasa Terrane is juvenile, similar to the Indochina data from our study (Fig. 5b; Ma et al., 2017). However, the data from this study, when integrated with published works in Fig. 6, highlights a distinct isotopic contrast between juvenile western Indochina and the evolved Truong Son Belt, which are both part of the composite Indochina Terrane. Previous studies in the northern Truong Son Belt (see Fig. 6; Liu et al., 2012; Wang et al., 2016b) produced $\varepsilon Hf_{(t)}$ and $\varepsilon Nd_{(t)}$ values that were generally negative and had corresponding T_{DM} ages dated to the Paleoproterozoic and backed up by zircon U—Pb inheritance ages. Further south in the Truong Son Belt, the $\varepsilon Nd_{(t)}$ values from Hoa et al. (2008) range from +6 for in extrusive rocks from Dak Lin to −13.3 for the peraluminous granite from Hai Van Complex. Hoa et al. (2008) stated that the model ages for the Permo-Triassic granites in this study were late Paleoproterozoic (2.23 to 1.80 Ga). Although these model ages are older than the T_{DM} for the Indochina Terrane determined in this study, much of the isotopic data from the Truong Son Belt is comparable (see Fig. 5b and c). The main isotopic difference is that along with the juvenile signature observed in both Indochina and Truong Son, Truong Son also has a more evolved component, which is coincidentally similar to values seen in the Sukhothai Terrane. A more comprehensive study of Indochina, its western margin, the Truong Son Belt and the regions through Cambodia and Laos, is required to further understand this relationship.

South China and Indochina have been shown in a previous detrital U—Pb zircon provenance study to be statistically similar with Gondwanan elements, common sediment sources and palaeo-proximity (Burrett et al., 2014). In the South China Terrane, Permo-Triassic granitoids with $\varepsilon Nd_{(t)}$ values of −11 to −8 and T_{DM} values of 2.0 to 1.6 Ga, have been interpreted to be derived from Neoproterozoic sedimentary and igneous rocks based on zircon inheritance and the spatial relationship to adjacent Neoproterozoic material (Gao et al., 2017). This supports the idea that Indochina was spatially linked with South China in the Neoproterozoic, possibly part of the geodynamic system involving South China, Madagascar, NW India and Seychelles presented by Wang et al. (2017). This study produced new isotopic data and has incorporated all the available published $\varepsilon Nd_{(t)}$ and recalculated $\varepsilon Hf_{(t)}$ data from Thailand and neighbouring regions of Myanmar, Laos, China and Vietnam to visualise and highlight trends in the isotopic characteristics. However, more analysis of the separate components of the composite Indochina and South China terranes, would be beneficial in order to constrain their affinities and palaeo-positions more closely.

The young and juvenile Indochina Terrane contrasts with the Sibumasu Terrane, which is more conceivably part of ancient cratonic Australia. The T_{DM} ages of the Sibumasu Terrane are within the range of values also seen in Western Australia through the Kimberley, Pilbara and Yilgarn regions (McCulloch, 1987; Wilde, 1999). For example, Sibumasu may have originated outboard of northwest Australia, in association with the Barramundi and older orogens (Ali et al., 2013; Bunopas, 1981; Burrett et al., 2014; McCulloch, 1987; Sevastjanova et al., 2016).

In this study, we demonstrate that the Sukhothai arc system involved pre-Paleozoic continental crust, contrary to models where Sukhothai represents a Carboniferous oceanic arc system (Sone and Metcalfe, 2008). Possible explanations for these observations include: 1) The Sukhothai arc would have been located outboard of Sibumasu on the northwest Australian margin of Gondwana (see Fig. 7). In this model, the Inthanon Zone would represent the back-arc basin between Sibumasu and Sukhothai and the main Palaeo-Tethys suture would separate Sukhothai and Indochina (the Nan Suture). 2) The Sukhothai arc was derived from Indochina, but contains relict Precambrian signatures, similar to those signatures observed in the Truong Son Belt to the northeast. This would require a zone of weakness between the more juvenile western Thai Indochina Terrane and the evolved Sukhothai Terrane crust to have been exploited by the back-arc extension that separated these terranes (see Fig. 7). For example, analogue modelling by Corti et al. (2013) has shown how the boundary zone between colder, more rigid cratonic (i.e. Archean-type) crust, and less rigid mobile belts tends to localise rifting.

Explanation 1) is contrary to popular models where the Inthanon Zone represents the main Palaeo-Tethys suture. These models are based on the presence of long-lived Devonian–Triassic highly condensed deep marine cherts, allochthonous limestone-capped seamounts and the continuation of the zone into the Changning–Menglian zone of Yunnan (see reviews in Sone and Metcalfe, 2008; Metcalfe, 2013; Gardiner et al., 2016). Explanation 2) adheres to the currently accepted consensus regarding the origin of the terranes, but requires a coincidence of circumstances to explain the lack of similarity between the Sukhothai and Indochina terranes. However, there is a third possibility that may reconcile these two contradictory explanations. The hybridised nature of the mid-Triassic granitoids in the Sukhothai Terrane may be due to the incorporation of evolved distal passive margin sequences of the Sibumasu Terrane as they approached the subduction zone (see illustration in Fig. 7). A similar manner of arc contamination is observed in the Sunda Arc (Handley et al., 2011). In this third model, the Sukhothai Terrane could still be part of the Indochina Terrane and the Inthanon Zone could still represents the major Palaeo-Tethys suture, coinciding with the evidence from the long-lived deep basin sedimentary sequences. It also broadly follows the geochemical data from the Sukhothai Terrane that appears to spatially distinguish between the I-type and hybrid granites, with more juvenile granitoids closer to the margin with Indochina and more crustal contamination in the granites further west, closer to the Inthanon Zone boundary. Nevertheless, further analyses and data collation on a regional scale is required to visualise a more complete history of the founding components of Southeast Asia.

7. Conclusion

This study used granites as a probe to further develop our understanding of the unexposed basement in Thailand. From the investigation of zircon U—Pb geochronology and Lu—Hf isotopic systems and whole-rock Sm—Nd, Sr and Pb geochemistry of granitoids, we determined:

- The Indochina Terrane is isotopically juvenile
- The Sukhothai Terrane has a hybridised isotopic signature indicating that juvenile material was contaminated with evolved continental crust
- The Sibumasu Terrane and associated Inthanon Zone contain relatively evolved, recycled crust

- εHf–$Nd_{(t)}$ model highlights a trend from evolved granitoid source material in the west of Thailand (Sibumasu and Inthanon) through to juvenile affinities in the east (Indochina)

Contrary to a number of previous hypotheses, the Indochina Terrane is built on relatively juvenile crust that formed primarily in the Neoproterozoic. There is no evidence for older crust in the western part of the Indochina Terrane. This contrasts with the Sibumasu and Sukhothai terranes that preserve evolved crustal material. We suggest that the hybridised isotopic nature of the mid-Triassic granitoids in the Sukhothai Terrane is due to the integration of evolved material from the Sibumasu Terrane during the progressive subduction of the Palaeo-Tethys Ocean.

Funding

This work was supported by Australian Research Council [#DP150101730, #DP120101460 and #FT120100340]. RECD is also funded by a University of Adelaide Research Training Program Stipend and some of the fieldwork conducted was funded on an Endeavour Australia Cheung Kong Fellowship. P. Kanjanapayont is funded by the Ratchadaphiseksomphot Endowment Fund, Chulalongkorn University. SN is funded by a PhD fellowship of the Research Foundation Flanders (FWO). GeoHistory Facility instruments were funded via an Australian Geophysical Observing System grant provided to AuScope Pty Ltd. by the AQ44 Australian Education Investment Fund program. The NPII multi-collector was obtained via funding from the Australian Research Council LIEF program [#LE150100013].

Acknowledgements

Fieldwork was conducted with the kind assistance of staff and students from Chulalongkorn University and Chiang Mai University. Other field expeditions were conducted with great thanks to Liviu Matenco and Ernst Willingshofer from Utrecht University, Thamfatt Ng and Diew. Pîi Roj from Chiang Mai University Lapidary for training and permission to use facilities. We would like to acknowledge Ann-Eline Debeer from Ghent University for the zircon mount preparation for the KM, ST and NT samples. Many thanks to David Bruce from the University of Adelaide's Isotope Geochemistry Facility for his support in the whole-rock geochemistry component of this project along with Sarah Gilbert and Aoife McFadden at Adelaide Microscopy for their help with the zircon analyses. Also thanks to Stanley Mertzman at Franklin and Marshall College for analysing the major and trace elements for this research. Thank you to Brad McDonald at the GeoHistory Facility at Curtin University for instrument setup for the Hf analyses. Appreciation to Sheree Armistead for conducting the Hf analysis for the KM-20 sample and assistance with MATLAB. This is a contribution to IGCP projects #589 (Development of the Asian Tethyan Realm) and #628 (The Gondwana Map). This publication forms TRaX Record #411.

References

Ahrendt, H., Chonglakmani, C., Hansen, B.T., Helmcke, D., 1993. Geochronological cross section through northern Thailand. Journal of Southeast Asian Earth Sciences 8, 207–217.

Ali, J.R., Cheung, H.M.C., Aitchison, J.C., Sun, Y., 2013. Palaeomagnetic re-investigation of Early Permian rift basalts from the Baoshan Block, SW China: constraints on the site-of-origin of the Gondwana-derived eastern Cimmerian terranes. Geophysical Journal International 193, 650–663.

Arboit, F., Collins, A.S., King, R., Morley, C.K., Hansberry, R., 2014. Structure of the Sibumasu–Indochina collision, central Thailand: A section through the Khao Khwang Fold and thrust belt. Journal of Asian Earth Sciences 95, 182–191.

Arboit, F., Collins, A.S., Jourdan, F., King, R., Foden, J., Amrouch, K., 2016. Geochronological and geochemical study of mafic and intermediate dykes from the Khao Khwang Fold-Thrust Belt: Implications for petrogenesis and tectonic evolution. Gondwana Research 36, 111–128.

Arndt, N.T., Goldstein, S.L., 1987. Use and abuse of crust-formation ages. Geology 15, 893–895.

Audley-Charles, M.G., Ballantyne, P.D., Hall, R., 1988. Mesozoic-Cenozoic rift-drift sequence of Asian fragments from Gondwanaland. Tectonophysics 155, 317–330.

Barber, A.J., Ridd, M.F., Crow, M.J., 2011. The origin, movement and assembly of the pre-Tertiary tectonic units of Thailand. In: Ridd, M.F., Barber, A.J., Crow, M.J. (Eds.), The Geology of Thailand. The Geological Society, London, pp. 507–537.

Barovich, K.M., Patchett, P.J., 1992. Behavior of isotopic systematics during deformation and metamorphism: a Hf, Nd and Sr isotopic study of mylonitized granite. Contributions to Mineralogy and Petrology 109, 386–393.

Barr, S.M., Macdonald, A.S., 1987. Nan River suture zone, northern Thailand. Geology 15, 907–910.

Barr, S.M., Macdonald, A.S., 1991. Toward a late Palaeozoic–early Mesozoic tectonic model for Thailand. Journal of Thai Geoscience 1, 11–22.

Barr, S.M., Macdonald, A.S., Ounchanum, P., Hamilton, M.A., 2006. Age, tectonic setting and regional implications of the Chiang Khong volcanic suite, northern Thailand. Journal of the Geological Society 163, 1037–1046.

Beckinsale, R.D., Suensilpong, S., Nakapadungrat, S., Walsh, J.N., 1979. Geochronology and geochemistry of granite magmatism in Thailand in relation to a plate tectonic model. Journal of the Geological Society 136, 529–537.

Blades, M.L., Collins, A.S., Foden, J., Payne, J.L., Xu, X., Alemu, T., Woldetinsae, G., Clark, C., Taylor, R.J.M., 2015. Age and hafnium isotopic evolution of the Didesa and Kemashi Domains, western Ethiopia. Precambrian Research 270, 267–284.

Booth, J., Sattayarak, N., 2011. Subsurface Carboniferous - Cretaceous geology of NE Thailand. In: Ridd, M.F., Barber, A.J., Crow, M.J. (Eds.), The Geology of Thailand. The Geological Society, London, pp. 185–222.

Bunopas, S., 1981. Paleogeographic history of western Thailand and adjacent parts of Southeast Asia - A plate tectonics interpretation. Paleogeographic History of Western Thailand and Adjacent Parts of Southeast Asia - A Plate Tectonics Interpretation.

Burrett, C., Khin, Z., Meffre, S., Lai, C.K., Khositanont, S., Chaodumrong, P., Udchachon, M., Ekins, S., Halpin, J., 2014. The configuration of Greater Gondwana—Evidence from LA ICPMS, U–Pb geochronology of detrital zircons from the Palaeozoic and Mesozoic of Southeast Asia and China. Gondwana Research 26, 31–51.

Cai, F., Ding, L., Yao, W., Laskowski, A.K., Xu, Q., Zhang, J.e., Sein, K., 2017. Provenance and tectonic evolution of Lower Paleozoic–Upper Mesozoic strata from Sibumasu terrane. Myanmar. Gondwana Research 41, 325–336.

Chaodamrong, P., 1992. Stratigraphy, Sedimentology and Tectonic Implications of the Lampang Group, Central North Thailand. Geology. University of Tasmania, Hobart, p. 230.

Chappell, B.W., White, A.J.R., 1992. I- and S-type granites in the Lachlan Fold Belt. In: Brown, P.E., Chappell, B.W. (Eds.), The Second Hutton Symposium on the Origin of Granites and Related Rocks. Geological Society of America.

Chappell, B.W., White, A.J.R., 2001. Two contrasting granite types: 25 years later. Australian Journal of Earth Sciences 48, 489–499.

Charusiri, P., Clark, A.H., Farrar, E., Archibald, D., Charusiri, B., 1993. Granite belts in Thailand: evidence from the 40Ar/39Ar geochronological and geological syntheses. Journal of Southeast Asian Earth Sciences 8, 127–136.

Cobbing, E.J., 2011. Granitic Rocks. In: Ridd, M.F., Barber, A.J., Crow, M.J. (Eds.), The Geology of Thailand. The Geological Society, London, pp. 443–457.

Cobbing, E.J., Pitfield, P.E.J., Darbyshire, P.D.F., Mallick, D.I.J., 1992. Thailand, The Granites of the South-East Asian Tin Belt. HMSO, London.

Cocks, L.R.M., Torsvik, T.H., 2013. The dynamic evolution of the Palaeozoic geography of eastern Asia. Earth-Science Reviews 117, 40–79.

Collins, A.S., 2003. Structure and age of the northern Leeuwin Complex, Western Australia: Constraints from field mapping and U–Pb isotopic analysis. Australian Journal of Earth Sciences 50, 585–599.

Corti, G., Iandelli, I., Cerca, M., 2013. Experimental modeling of rifting at craton margins. Geosphere 9, 138–154.

Dew, R.E.C., Nachtergaele, S., Collins, A.S., Glorie, S., Foden, J., De Grave, J., Blades, M.L., Morley, C.K., Evans, N.J. and Alessio, B.L. (submitted). Analysis of the U–Pb geochronology and Lu–Hf system in zircon and whole-rock Sr, Sm–Nd and Pb isotopic systems for the granitoids of Thailand, Data in Brief.

Du, B., Wang, C., He, Z., Yang, L., Chen, J., Shi, K., Luo, Z., Xia, J., 2016. Advances in research of bulk-rock Nd and zircon Hf isotopic mappings: Case study of Sanjiang Tethyan Orogen. Acta Petrologica Sinica 32, 2555–2570.

Faure, M., Lepvrier, C., Nguyen, V.V., Vu, T.V., Lin, W., Chen, Z., 2014. The South China block-Indochina collision: Where, when, and how. Journal of Asian Earth Sciences 79, 260–274.

Fletcher, I.R., Libby, W.G., 1993. Further Isotopic Evidence for the Existence of Two Distinct Terranes in the Southern Pinjarra Orogen. Professional Papers. Geological Survey, Western Australia, Western Australia, pp. 81–83.

Gao, P., Zheng, Y.-F., Zhao, Z.-F., 2017. Triassic granites in South China: A geochemical perspective on their characteristics, petrogenesis, and tectonic significance. Earth-Science Reviews 173, 266–294.

Gardiner, N.J., Searle, M.P., Morley, C.K., Whitehouse, M.P., Spencer, C.J., Robb, L.J., 2016. The closure of Palaeo-Tethys in Eastern Myanmar and Northern Thailand: New insights from zircon U-Pb and Hf isotope data. Gondwana Research 39, 401–422.

Ghosh, S., Fallick, A.E., Paul, D.K., Potts, P.J., 2005. Geochemistry and Origin of Neoproterozoic Granitoids of Meghalaya, Northeast India: Implications for Linkage with Amalgamation of Gondwana Supercontinent. Gondwana Research 8, 421–432.

Goldstein, S.L., O'Nions, R.K., Hamilton, P.J., 1984. A Sm-Nd isotopic study of atmospheric dusts and particulates from major river systems. Earth and Planetary Science Letters 70, 221–236.

Griffin, W., Wang, X., Jackson, S., Pearson, N., O'Reilly, S.Y., Xu, X., Zhou, X., 2002. Zircon chemistry and magma mixing, SE China: insitu analysis of Hf isotopes, Tonglu and Pingtan igneous complexes. Lithos 61, 237–269.

Halpin, J.A., Tran, H.T., Lai, C.-K., Meffre, S., Crawford, A.J., Zaw, K., 2016. U–Pb zircon geochronology and geochemistry from NE Vietnam: A 'tectonically disputed' territory between the Indochina and South China blocks. Gondwana Research 34, 254–273.
Handley, H.K., Turner, S., Macpherson, C.G., Gertisser, R., Davidson, J.P., 2011. Hf–Nd isotope and trace element constraints on subduction inputs at island arcs: Limitations of Hf anomalies as sediment input indicators. Earth and Planetary Science Letters 304, 212–223.
Hansen, B.T., Wemmer, K., 2011. Age and evolution of the basement in Thailand. In: Ridd, M.F., Barber, A.J., Crow, M.J. (Eds.), The Geology of Thailand. The Geological Society, London, pp. 19–32.
Hara, H., Kunii, M., Hisada, K.I., Ueno, K., Kamata, Y., Srichan, W., Charusiri, P., Charoentitirat, T., Watarai, M., Adachi, Y., Kurihara, T., 2012. Petrography and geochemistry of clastic rocks within the Inthanon zone, northern Thailand: Implications for Paleo-Tethys subduction and convergence. Journal of Asian Earth Sciences 61, 2–15.
Hara, H., Kon, Y., Usuki, T., Lan, C.Y., Kamata, Y., Hisada, K.I., Ueno, K., Charoentitirat, T., Charusiri, P., 2013. U-Pb ages of detrital zircons within the Inthanon Zone of the Paleo-Tethyan subduction zone, northern Thailand: New constraints on accretionary age and arc activity. Journal of Asian Earth Sciences 74, 50–61.
Hara, H., Kunii, M., Miyake, Y., Hisada, K.I., Kamata, Y., Ueno, K., Kon, Y., Kurihara, T., Ueda, H., Assavapatchara, S., Treerotchananon, A., Charoentitirat, T., Charusiri, P., 2017. Sandstone provenance and U–Pb ages of detrital zircons from Permian–Triassic forearc sediments within the Sukhothai Arc, northern Thailand: Record of volcanic-arc evolution in response to Paleo-Tethys subduction. Journal of Asian Earth Sciences 146, 30–55.
Hart, S.R., 1984. A large-scale isotope anomaly in the Southern Hemisphere mantle. Nature 309, 753–757.
Hisada, K.-i., Sugiyama, M., Ueno, K., Charusiri, P., Arai, S., 2004. Missing ophiolitic rocks along the Mae Yuam Fault as the Gondwana–Tethys divide in north-west Thailand. Island Arc 13, 119–127.
Hoa, T.T., Anh, T.T., Phuong, N.T., Dung, P.T., Anh, T.V., Izokh, A.E., Borisenko, A.S., Lan, C.Y., Chung, S.L., Lo, C.H., 2008. Permo-Triassic intermediate–felsic magmatism of the Truong Son belt, eastern margin of Indochina. Comptes Rendus Geoscience 340, 112–126.
Intasopa, S., Dunn, T., 1994. Petrology and SrNd isotopic systems of the basalts and rhyolites, Loei, Thailand. Journal of Southeast Asian Earth Sciences 9, 167–180.
Javanaphet, C., 1969. Geological Map of Thailand; Scale 1 : 1 000 000, with explanation. Department of Mineral Resources, Bangkok.
Jiang, H., Li, W.-Q., Jiang, S.-Y., Wang, H., Wei, X.-P., 2017. Geochronological, geochemical and Sr-Nd-Hf isotopic constraints on the petrogenesis of Late Cretaceous A-type granites from the Sibumasu Block, Southern Myanmar, SE Asia. Lithos 268–271, 32–47.
Kamvong, T., Khin, Z., Meffre, S., Maas, R., Stein, H., Lai, C.-K., 2014. Adakites in the Truong Son and Loei fold belts, Thailand and Laos: Genesis and implications for geodynamics and metallogeny. Gondwana Research 26, 165–184.
Kanjanapayont, P., Klötzli, U., Thöni, M., Grasemann, B., Edwards, M.A., 2012. Rb–Sr, Sm–Nd, and U–Pb geochronology of the rocks within the Khlong Marui shear zone. southern Thailand. Journal of Asian Earth Sciences 56, 263–275.
Kawakami, T., Nakano, N., Higashino, F., Hokada, T., Osanai, Y., Yuhara, M., Charusiri, P., Kamikubo, H., Yonemura, K., Hirata, T., 2014. U-Pb zircon and CHIME monazite dating of granitoids and high-grade metamorphic rocks from the Eastern and Peninsular Thailand — A new report of Early Paleozoic granite. Lithos 200–201, 64–79.
Kemp, A.I.S., Hawkesworth, C.J., Paterson, B.A., Kinny, P.D., 2006. Episodic growth of the Gondwana supercontinent from hafnium and oxygen isotopes in zircon. Nature 439, 580–583.
Kong, S., Watanabe, K., Imai, A., 2012. Magnetic susceptibility and geochemistry of granitic rocks in Cambodia. ASEAN Engineering Journal Part C 2, 113–132.
Lan, C.Y., Chung, S.L., Van Long, T., Lo, C.H., Lee, T.-Y., Mertzman, S.A., Shen, J.J.-S., 2003. Geochemical and Sr–Nd isotopic constraints from the Kontum massif, central Vietnam on the crustal evolution of the Indochina block. Precambrian Research 7–27.
Lepvrier, C., Maluski, H., Van Tich, V., Leyreloup, A., Truong Thi, P., Van Vuong, N., 2004. The Early Triassic Indosinian orogeny in Vietnam (Truong Son Belt and Kontum Massif); implications for the geodynamic evolution of Indochina. Tectonophysics 393, 87–118.
Li, P., Rui, G., Junwen, C., Ye, G., 2004. Paleomagnetic analysis of eastern Tibet: implications for the collisional and amalgamation history of the Three Rivers Region. SW China. Journal of Asian Earth Sciences 24, 291–310.
Liew, T.C., McCulloch, M.T., 1985. Genesis of granitoid batholiths of Peninsular Malaysia and implications for models of crustal evolution: Evidence from a NdSr isotopic and UPb zircon study. Geochimica et Cosmochimica Acta 49, 587–600.
Lin, Y.-L., Yeh, M.-W., Lee, T.-Y., Chung, S.-L., Iizuka, Y., Charusiri, P., 2013. First evidence of the Cambrian basement in Upper Peninsula of Thailand and its implication for crustal and tectonic evolution of the Sibumasu terrane. Gondwana Research 24, 1031–1037.
Liu, J., Tran, M.-D., Tang, Y., Nguyen, Q.-L., Tran, T.-H., Wu, W., Chen, J., Zhang, Z., Zhao, Z., 2012. Permo-Triassic granitoids in the northern part of the Truong Son belt, NW Vietnam: Geochronology, geochemistry and tectonic implications. Gondwana Research 22, 628–644.
Ludwig, K.R., 1998. On the Treatment of Concordant Uranium-Lead Ages. Geochimica et Cosmochimica Acta 62, 665–676.
Ma, X., Xu, Z., Meert, J.G., 2017. Syn-convergence extension in the southern Lhasa terrane: Evidence from late Cretaceous adakitic granodiorite and coeval gabbroic-dioritic dykes. Journal of Geodynamics 110, 12–30.
Mahawat, C., Atherton, M.P., Brotherton, M.S., 1990. The Tak Batholith, Thailand: the evolution of contrasting granite types and implications for tectonic setting. Journal of Southeast Asian Earth Sciences 4, 11–27.
McCulloch, M.T., 1987. Sm-Nd isotopic constraints on the evolution of Precambrian crust in the Australian continent. In: Kröner, A. (Ed.), Proterozoic lithospheric evolution. American Geophysical Union, Washington, D.C., pp. 115–130.
Meffre, S., Khin, Z., Khositanont, S., Halpin, J., Cumming, G., 2008. 'Tectonic evolution of SE Asia', 'Ore Deposits of SE Asia'. Annual Report to Sponsors. CODES. Hobart, Australia.
Metcalfe, I., 1984. Stratigraphy, palaeontology and palaeogeography of the Carboniferous of Southeast Asia. Memoires de la Societe Geologique de France 147, 107–118.
Metcalfe, I., 2013. Gondwana dispersion and Asian accretion: Tectonic and palaeogeographic evolution of eastern Tethys. Journal of Asian Earth Sciences 66, 1–33.
Mitchell, A.H.G., 1992. Late Permian-Mesozoic events and the Mergui Group Nappe in Myanmar and Thailand. Journal of Southeast Asian Earth Sciences 7, 165–178.
Morley, C.K., Ampaiwan, P., Thanudamrong, S., Kuenphan, N., Warren, J., 2013. Development of the Khao Khwang fold and thrust belt; implications for the geodynamic setting of Thailand and Cambodia during the Indosinian Orogeny. Journal of Asian Earth Sciences 62, 705–719.
Nakano, N., Osanai, Y., Nam, N.V., Tri, T.V., 2018. Bauxite to eclogite: Evidence for late Permian supracontinental subduction at the Red River shear zone, northern Vietnam. Lithos 302–303, 37–49.
Ng, S.W., Chung, S.L., Robb, L.J., Searle, M.P., Ghani, A.A., Whitehouse, M.J., Oliver, G.J.H., Sone, M., Gardiner, N.J., Roselee, M.H., 2015a. Petrogenesis of Malaysian granitoids in the Southeast Asian tin belt: Part 1. Geochemical and Sr-Nd isotopic characteristics. Bulletin of the Geological Society of America 127, 1209–1237.
Ng, S.W., Whitehouse, M.J., Searle, M.P., Robb, L.J., Ghani, A.A., Chung, S.L., Oliver, G.J.H., Sone, M., Gardiner, N.J., Roselee, M.H., 2015b. Petrogenesis of Malaysian granitoids in the Southeast Asian tin belt: Part 2. U-Pb zircon geochronology and tectonic model. Bulletin of the Geological Society of America 127, 1238–1258.
Patchett, P.J., Tatsumoto, M., 1980. Hafnium isotope variations in oceanic basalts. Geophysical Research Letters 7, 1077–1080.
Pour, A.B., Hashim, M., Park, Y., 2017. Gondwana-Derived Terranes Structural Mapping Using PALSAR Remote Sensing Data. Journal of the Indian Society of Remote Sensing 1–14.
Qian, X., Feng, Q., Wang, Y., Chonglakmani, C., Monjai, D., 2016. Geochronological and geochemical constraints on the mafic rocks along the Luang Prabang zone: Carboniferous back-arc setting in northwest Laos. Lithos 245, 60–75.
Qian, X., Feng, Q., Wang, Y., Zhao, T., Zi, J.-W., Udchachon, M., Wang, Y., 2017. Late Triassic post-collisional granites related to Paleotethyan evolution in SE Thailand: Geochronological and geochemical constraints. Lithos 286, 440–453.
Ridd, M.F., 2011. Lower Palaeozoic. In: Ridd, M.F., Barber, A.J., Crow, M.J. (Eds.), The Geology of Thailand. The Geological Society, London, pp. 33–51.
Romer, R.L., Förster, H.-J., Hahne, K., 2012. Strontium isotopes — A persistent tracer for the recycling of Gondwana crust in the Variscan orogen. Gondwana Research 22, 262–278.
Salam, A.A., Zaw, K., Meffre, S., McPhie, J., Lai, C.-K., 2014. Geochemistry and geochronology of the Chatree epithermal gold-silver deposit: Implications for the tectonic setting of the Loei Fold Belt, central Thailand. Gondwana Research 26, 198–217.
Schwartz, M.O., Rajah, S.S., Askury, A.K., Putthapiban, P., Djaswadi, S., 1995. The Southeast Asian tin belt. Earth-Science Reviews 38, 95–293.
Searle, M.P., Whitehouse, M.J., Robb, L.J., Ghani, A.A., Hutchison, C.S., Sone, M., Ng, S.W.P., Roselee, M.H., Chung, S.L., Oliver, G.J.H., 2012. Tectonic evolution of the Sibumasu-Indochina terrane collision zone in Thailand and Malaysia: Constraints from new U-Pb zircon chronology of SE Asian tin granitoids. Journal of the Geological Society 169, 489–500.
Sevastjanova, I., Clements, B., Hall, R., Belousova, E.A., Griffin, W.L., Pearson, N., 2011. Granitic magmatism, basement ages, and provenance indicators in the Malay Peninsula: Insights from detrital zircon U–Pb and Hf-isotope data. Gondwana Research 19, 1024–1039.
Sevastjanova, I., Hall, R., Rittner, M., Paw, S.M.T.L., Naing, T.T., Alderton, D.H., Comfort, G., 2016. Myanmar and Asia united, Australia left behind long ago. Gondwana Research 32, 24–40.
Shi, M.F., Lin, F.C., Fan, W.Y., Deng, Q., Cong, F., Tran, M.D., Zhu, H.P., Wang, H., 2015. Zircon U-Pb ages and geochemistry of granitoids in the Truong Son terrane, Vietnam: Tectonic and metallogenic implications. Journal of Asian Earth Sciences 101, 101–120.
Singharajwarapan, S., Berry, R., 2000. Tectonic implications of the Nan Suture Zone and its relationship to the Sukhothai Fold Belt, Northern Thailand. Journal of Asian Earth Sciences 18, 663–673.
Sone, M., Metcalfe, I., 2008. Parallel Tethyan sutures in mainland Southeast Asia: New insights for Palaeo-Tethys closure and implications for the Indosinian orogeny. Comptes Rendus - Geoscience 340, 166–179.
Sone, M., Metcalfe, I., Chaodumrong, P., 2012. The Chanthaburi terrane of southeastern Thailand: Stratigraphic confirmation as a disrupted segment of the Sukhothai Arc. Journal of Asian Earth Sciences 61, 16–32.
Stacey, J.S., Kramers, J.D., 1975. Approximation of terrestrial lead isotope evolution by a two-stage model. Earth and Planetary Science Letters 26, 207–221.
Taylor, R.N., Ishizuka, O., Michalik, A., Milton, J.A., Croudace, I.W., 2015. Evaluating the precision of Pb isotope measurement by mass spectrometry. Journal of Analytical Atomic Spectrometry 30, 198–213.
Ueno, K., Charoentitirat, T., 2011. Carboniferous and Permian. In: Ridd, M.F., Barber, A.J., Crow, M.J. (Eds.), The Geology of Thailand. The Geological Society, London, pp. 71–136.
Ueno, K., Hisada, K., 2001. The Nan-Uttaradit-Sa Kaeo Suture as a main Paleo-Tethyan suture in Thailand: Is it real. Gondwana Research, pp. 804–805.
Usuki, T., Lan, C.-Y., Wang, K.-L., Chiu, H.-Y., 2013. Linking the Indochina block and Gondwana during the Early Paleozoic: Evidence from U–Pb ages and Hf isotopes of detrital zircons. Tectonophysics 586, 145–159.

Vervoort, J.D., Patchett, P.J., Blichert-Toft, J., Albarède, F., 1999. Relationships between Lu–Hf and Sm–Nd isotopic systems in the global sedimentary system. Earth and Planetary Science Letters 168, 79–99.
Wakita, K., Metcalfe, I., 2005. Ocean Plate Stratigraphy in East and Southeast Asia. Journal of Asian Earth Sciences 24, 679–702.
Wang, L., Long, W., Zhou, D., Xu, W., Jin, X., 2016a. Late Triassic zircon U-Pb ages and Sr-Nd-Hf isotopes of Darongshan granites in southeastern Guangxi and their geological implications. Geological Bulletin of China 35, 1291–1303.
Wang, S., Mo, Y., Wang, C., Ye, P., 2016b. Paleotethyan evolution of the Indochina Block as deduced from granites in northern Laos. Gondwana Research 38, 183–196.
Wang, Y., He, H., Cawood, P.A., Srithai, B., Feng, Q., Fan, W., Zhang, Y., Qian, X., 2016c. Geochronological, elemental and Sr-Nd-Hf-O isotopic constraints on the petrogenesis of the Triassic post-collisional granitic rocks in NW Thailand and its Paleotethyan implications. Lithos 266 (267), 264–286.
Wang, W., Cawood, P.A., Zhou, M.-F., Pandit, M.K., Xia, X.-P., Zhao, J.-H., 2017. Low-δ18O Rhyolites From the Malani Igneous Suite: A Positive Test for South China and NW India Linkage in Rodinia. Geophysical Research Letters 44, 10,298–210,305.
Wielchowsky, C.C., Young, J.D., 1985. Regional facies variations in Permian rocks of the Phetchabun fold and thrust belt, Thailand. In: Thanvarachorn, P., Hokjaroen, S., Youngme, W. (Eds.), Conference on Geology and Mineral Resources Development of the North-east Thailand, Khon Kaen, pp. 41–55.
Wilde, S.A., 1999. Evolution of the Western Margin of Australia during the Rodinian and Gondwanan Supercontinent Cycles. Gondwana Research 2, 481–499.
Yokart, B., Barr, S.M., Williams-Jones, A.E., Macdonald, A.S., 2003. Late-stage alteration and tin–tungsten mineralization in the Khuntan Batholith, northern Thailand. Journal of Asian Earth Sciences 21, 999–1018.
Zaw, K., Meffre, S., Lai, C.-K., Burrett, C., Santosh, M., Graham, I., Manaka, T., Salam, A., Kamvong, T., Cromie, P., 2014. Tectonics and metallogeny of mainland Southeast Asia — A review and contribution. Gondwana Research 26, 5–30.